# Cripto regulates skeletal muscle regeneration and modulates satellite cell determination by antagonizing myostatin.

Ombretta Guardiola, Peggy Lafuste, Silvia Brunelli, Salvatore Iaconis, Thierry Touvier, Philippos Mourikis, Katrien de Bock, Enza Lonardo, Gennaro Andolfi, Ann Bouché, et al.

*Classification:* Biological Sciences, Developmental Biology;

# CRIPTO REGULATES SKELETAL MUSCLE REGENERATION AND MODULATES SATELLITE CELL DETERMINATION BY ANTAGONIZING MYOSTATIN

Ombretta Guardiola[1,2*], Peggy Lafuste[3,4,5,*], Silvia Brunelli[6,7,§], Salvatore Iaconis[1,2,§], Thierry Touvier[8], Philippos Mourikis[9], Katrien De Bock[3,4], Enza Lonardo[1,2], Gennaro Andolfi[1,2], Ann Bouché[3], Giovanna L. Liguori[2], Michael M. Shen[10], Shahragim Tajbakhsh[9], Giulio Cossu[11], Peter Carmeliet[3,4,‡] and Gabriella Minchiotti[1,2‡^]

1. Stem Cell Fate Laboratory, Institute of Genetics and Biophysics "A. Buzzati Traverso", CNR, Naples 80131, Italy.

2. Institute of Genetics and Biophysics "A. Buzzati Traverso", CNR, Naples 80131, Italy.

3. Vesalius Research Center, VIB, Leuven 3000, Belgium;

4. Vesalius Research Center, K.U.Leuven, Leuven 3000, Belgium

5. INSERM, U955, team 10 "Cell interactions in the neuromuscular system", University Paris Est Creteil, F-94000 Creteil, France.

6. Division of Regenerative Medicine, San Raffaele Scientific Institute, 20132 Milan, Italy.

7. Department of Experimental Medicine, University of Milano-Bicocca, 20052, Monza, Italy

8. E Medea Scientific Institute, 23842 Bosisio Parini, Italy

9. Institut Pasteur, Stem Cells & Development, CNRS URA 2578, Paris, France

10. Columbia University College of Physicians and Surgeons Herbert Irving Comprehensive Cancer Center, New York, NY 10032

11. Department of Cell and Developmental Biology, University College London. WC1E 6DE, United Kingdom

Running Title: Role of Cripto in skeletal muscle regeneration

* Equally contributed as co-first author. § Equally contributed as co-second author

‡ Equally contributed as co-last author

^ Corresponding author: Gabriella Minchiotti
Stem Cell Fate Laboratory
Institute of Genetics and Biophysics “A. Buzzati-Traverso”, CNR
Via Pietro Castellino 111
80131 Naples, Italy
Tel. 0039 081 6132357; Fax 0039 081 6132595
gabriella.minchiotti@igb.cnr.it

**SUMMARY**

Skeletal muscle regeneration mainly depends on satellite cells, a population of resident muscle stem cells. Yet, our understanding of the molecular mechanisms underlying satellite cell activation is still largely undefined. Here, we show that Cripto, a regulator of early embryogenesis, is a novel regulator of muscle regeneration and satellite cell progression toward the myogenic lineage. Conditional inactivation of *cripto* in adult satellite cells compromises skeletal muscle regeneration, whereas gain of function of Cripto accelerates regeneration leading to muscle hypertrophy. Moreover, we provide evidence that Cripto modulates myogenic cell determination and promotes proliferation by antagonizing the TGFβ ligand Myostatin. Our data provide new insights in the molecular and cellular basis of Cripto activity in skeletal muscle regeneration and raise novel implications for stem cell biology and regenerative medicine.

\body

## INTRODUCTION

It is now evident that genes and molecular mechanisms, which have key roles during embryogenesis, are reactivated in the adult during tissue remodeling and regeneration, and when deregulated may contribute to cancer progression (1). The *cripto* gene has emerged as a key player in this complex scenario. Cripto is a GPI-anchored protein and the founder member of a family of signaling molecules, the EGF-CFC proteins, important for vertebrate development (2). Cripto is associated with the pluripotent status of both human and mouse embryonic stem cells (ESCs) (3) and it acts as a key player in the signaling networks orchestrating ESC differentiation (4). Intriguingly, it has been recently suggested that Cripto may serve as regulator to control dormancy of hematopoietic stem cells (HSCs) (5).

Under normal physiological conditions, Cripto is expressed during embryonic development (2) and it has been shown to have activity both as a soluble factor and GPI-anchored protein (6-8). Existing models indicate that Cripto can function via different signaling pathways. Cripto plays distinct and opposing roles in modulating the activity of several transforming growth factor-beta (TGFβ) ligands. Indeed as an obligate co-receptor, Cripto binds Nodal and GDF1/GDF3 and stimulates signaling through the activin receptor complex composed of type I serine-threonine ActRIB (ALK4) and type II receptor (ActRII/ActRIIB) (9-11). Following receptor activation, the intracellular effectors Smad2 and/or Smad3 are phosphorylated and accumulate in the nucleus with Smad4 to mediate transcriptional response (12). In contrast to its co-receptor function, Cripto is able to antagonize signaling of other members of the TGFβ family, i.e. Activins and TGFβ. This inhibitory activity of Cripto results in reduced ability to form an active ActRII/ActRIB

receptor complex (13-15). Despite the well-described role of Cripto in early development and ESC differentiation, the role of this protein in post-natal life remains elusive. To date, *de novo* expression of Cripto has been associated with several epithelial cancers (16, 17), but its role in other pathological conditions such as injury or degenerative diseases has not been investigated. Given the physiological activity of Cripto in the instructive events of embryonic mesodermal commitment and differentiation (4), we hypothesized that Cripto expression might be reactivated in response to injury in mesenchymal tissues such as skeletal muscles.

Adult skeletal muscle has a generally low cellular turnover rate. However, in response to certain pathological conditions, it undergoes robust regeneration. Regeneration is mainly dependent on satellite cells, a population of resident stem cells that is in a quiescent state during muscle homeostasis. Upon injury or disease, satellite cells become activated, proliferate, migrate to the site of injury and either fuse to form multinucleated myotubes or re-establish a self-renewing pool of quiescent satellite cells (18). Quiescent satellite cells express the transcription factor Pax7, which is involved in myogenic specification (19, 20). Upon injury, activated satellite cells, start proliferating and expressing MyoD, whereas Pax7 expression is progressively reduced. Subsequently, expression of Myogenin and MRF4 (MRF family of transcription factors) are up-regulated as cells enter their terminal differentiation program. A fraction of activated cells down-regulates expression of MyoD and returns to cellular quiescence to maintain a pool of satellite cells (21). A delicate balance between satellite cell proliferation and exit from cell cycle, differentiation, and fusion is required for the correct muscle regeneration to occur. Although some signaling molecules have been found to play a crucial role in these processes (11), including hepatocyte growth factor [HGF; (22)], insulin-like growth factors [IGF; (23)], Myostatin (24)

and Wnts (25), the underlying molecular mechanisms of muscle regeneration remain largely undefined.

In the present study, we provide the first evidence that Cripto is re-expressed in adult skeletal muscle in response to injury and that this response correlates with and regulates muscle regeneration. We also show that Cripto is expressed in activated satellite cells, and promotes myogenic cell determination and proliferation by antagonizing TGFβ ligand Myostatin.

## RESULTS

### CRIPTO IS EXPRESSED DURING SKELETAL MUSCLE REGENERATION AND IN MYOGENIC CELLS IN VIVO AND EX VIVO

To evaluate whether Cripto is activated in adult tissues under pathological conditions, we performed double immunofluorescence analysis for Cripto and Laminin on normal adult skeletal muscle both during homeostasis and after cardiotoxin (CTX) induced injury. Cripto was undetectable in healthy uninjured muscles (Figures 1A-1C); in contrast, strong expression of Cripto was observed in the regenerating area both inside and outside of the basement membrane surrounding myofibers (Figures 1D-1F). Cripto expression was confirmed by flow cytometry (FACS) analysis (Figure S1A). Notably, expression of *cripto* progressively decreases during the regeneration process (Figures S1C and S1D-S1F). To assess whether different cell types that take part in the regeneration process expressed Cripto, we performed double staining with specific markers. Immunofluorescence analysis revealed that Cripto was expressed in myogenic cells as indicated by co-expression with MyoD (Figures 1G-1I). In addition, double staining with F4/80, a macrophage-specific membrane antigen, showed that Cripto was also expressed in inflammatory cells (Figures 1J-1L). FACS analysis on dissociated muscle cells confirmed indeed that at day 4 after CTX injection, 15.2% of Cripto positive cells are F4/80 positive (Figure S1B).

Expression of *cripto* during muscle regeneration and in satellite cell progeny after activation raised the intriguing possibility that *cripto* might play a role in regulating myogenic cell behavior. To address this issue in more detail, we used single myofiber preparations isolated from wild type myofibers (26) and performed a time course immunofluorescence analysis for Cripto, Pax7 and MyoD. Immediately after plating (T0), Cripto expression was undetectable in Pax7+/MyoD- satellite cells (Figures 2A-2E and

2A'-2E'). Interestingly, Cripto started to be detected along with Pax7 and MyoD (Figures 2F-2J and 2F'-2J') as early as after 24 hours (T24), persisting after 48 hours (T48) in culture (Figures 2K-2O and 2K'-2O'). We then extended our analysis using myofibers isolated from *Myf5*$^{nlacZ/+}$ mice (27), which express a nuclear localized *lacZ* (*nlacZ*) reporter gene targeted to the *Myf5* locus (28). Double staining for Cripto and β-gal showed Cripto expression along with β-gal expression (Figures S2A-S2D). Moreover, Cripto expression persisted in satellite cells detaching from the fibers after 60 hours in culture (Figures S2E-S2H and S2I-S2L).

Taken together, our data provide evidence that Cripto is expressed in activated satellite cells committed to the myogenic lineage, persisting in proliferating transient amplifying myoblasts.

## CONDITIONAL TARGETED DELETION OF *CRIPTO* IN ADULT SATELLITE CELLS AFFECTS SKELETAL MUSCLE REGENERATION

These results prompted us to evaluate whether Cripto might have a physiological role in skeletal muscle regeneration *in vivo,* using a loss of function approach. *Cripto* null mutants die during early embryonic development (29), we thus used a Cre-lox strategy to obtain conditional *cripto*-deletion in adult mice. Moreover, to distinguish between the relative roles of Cripto in inflammatory and satellite cells contribution during this process, we generated a novel mouse model for conditional inactivation of *cripto* in satellite cells, *Tg:Pax7-CreERT2::Cripto*$^{loxP/-}$ mice, by crossing *Cripto*$^{loxP/-}$ mice with a tamoxifen-inducible *Tg:Pax7-CreERT2* transgenic line (30). *Tg:Pax7-CreERT2::Cripto*$^{loxP/-}$ adult mice were treated with tamoxifen or vehicle, as control, once a day for 5 days; at day 4, TA muscles were injected locally with CTX and the effect on muscle regeneration was evaluated at day 4 and 15 after CTX injection (Figures 3A). To first verify the tissue-specific recombinase

activity of Cre, we isolated and genotyped the contralateral uninjured TA muscle and the bone marrow of both tamoxifen and vehicle –treated mice (Figure 3B). As expected, the *cripto*-deleted specific band was detected in the contralateral uninjured TA muscle of the tamoxifen-treated, but not the control mice. Notably, the *cripto*-deleted band was absent in the bone marrow genomic DNA (Figure 3B), thus confirming that *cripto* deletion occurred selectively in skeletal muscle cells. Accordingly, Cripto protein levels decreased in muscle tissue of tamoxifen-treated mice compared to control, at day 4 after injury, as shown by ELISA assays (Figure 3C). Using these mice, we stained sections of the CTX injected TA muscles with H&E to perform morphometric analysis (Figure 3D). Remarkably, the myofiber cross sectional area (CSA) was significantly reduced in the tamoxifen–treated mice compared to control (Figures 3E and 3F). Given that Cripto is expressed also in macrophages, our data provide the first direct evidence for a role of Cripto specifically in adult myogenic cells during skeletal muscle regeneration.

### CRIPTO OVEREXPRESSION ACCELERATES SKELETAL MUSCLE REGENERATION AND INDUCES MYOFIBER HYPERTROPHY *IN VIVO*

We next investigated whether Cripto might modulate acute skeletal muscle regeneration *in vivo*, using a gain-of-function approach. To do so, we generated a replication-deficient adenovirus, Ad-sCripto that can be used to overexpress a biologically active soluble Cripto (sCripto) protein (31) in skeletal muscle. We first evaluated whether sCripto was sufficiently expressed upon Ad-sCripto gene transfer by measuring Cripto protein levels both in muscles and serum. To this end, Tibialis anterior (TA) muscles were injected with CTX along with either Ad-sCripto or Ad-Control (encoding an empty vector); mice were sacrificed at different time points and sCripto serum levels were determined by using a sandwich ELISA-based assay. As early as 6 hours after virus injection, sCripto

was detectable in the serum of Ad-sCripto infected mice (≈ 5 ng/ml), which progressively decreased to reach a level of ≈1 ng/ml after 6 days (Figure S3A); by contrast, sCripto was undetectable in the serum of mice infected with Ad-Control. Finally, a dose-dependent Cripto overexpression was also detected in Ad-sCripto transduced muscles after 5 days, confirming that sCripto was efficiently expressed upon Ad-sCripto gene transfer (Figures S3B).

To analyze the overall effect of sCripto overexpression on muscle regeneration, we triggered skeletal muscle regeneration by injecting high doses of CTX (32) in wild-type TA muscles infected with Ad-Control or Ad-sCripto. Mice were killed 4, 8 and 22 days after CTX and adenovirus injection. We first verified Cripto overexpression in the serum and in the skeletal muscles by ELISA and immunofluorescence analysis, respectively (Figures S3C and S3D). Muscle sections were then stained with hematoxylin and eosin (H&E) for the morphological and morphometric analysis (Figure 4A); muscle regeneration was assessed and expressed as percentage of the area of centrally nucleated fibers compared to the total muscle section area (Figure 4B) at each time point. At day 4 after injections, we did not find any significant difference between Ad-control and Ad-sCripto–infected muscles (18.7 ± 3% after Ad-sCripto vs 19.9 ± 4.5% after Ad-Control; n=5; P=NS); by contrast, 8 days after the CTX injury, Ad-sCripto infected muscles clearly exhibited more robust regeneration than control (64 ± 11% after Ad-sCripto vs 15 ± 1.2% after Ad-Control; n=5 mice; **P=0.004; Figures 4A and 4B). By day 22 after injury, although the regeneration process was nearly completed in both conditions, muscle regeneration was still significantly improved in Ad-sCripto–treated mice (92 ± 4.6% after Ad-sCripto vs 76 ± 4.5% after Ad-Control; n=5 mice; *P=0.04; Figures 4A and 4B). Comparable results were obtained in models of less severe muscle damage, i.e. femoral artery ligation (MLI) and lower doses of CTX (Figures S4A-S4C). In accordance with these findings, muscles

overexpressing Cripto also showed reduced necrotic areas compared to controls (36 ± 11% after Ad-sCripto vs 85 ± 1.2% after Ad-Control; n=5 mice; **P=0.004; Figure 4C). Moreover, the accelerated regeneration was accompanied by high expression, in Ad-sCripto muscles, of neonatal Myosin Heavy Chain (nMyHC), a marker of muscle regeneration in the adult. Expression of nMyHC, analyzed by quantitative Real Time PCR (qRT-PCR), significantly increased in Ad-sCripto mice at day 8 (Figure 4D). Most remarkably, morphometric analysis (CSA) showed that Cripto overexpression increased myofiber size both at 8 and 22 days after the CTX injury (Figures 4E and 4F, respectively), and results were confirmed in the model of less severe muscle damage (Figure S4C).

Taken together, our data indicate that sCripto overexpression accelerates muscle regeneration and induces myofiber hypertrophy following acute skeletal muscle damage. Among the different processes active in muscle healing and regeneration, inflammation plays an important role. Since Cripto was also expressed in macrophages during regeneration (Figures 1J-1L), we compared the degree of inflammation in TA muscles transduced with Ad-sCripto and Ad-Control. Immunostaining for F4/80 followed by morphometric analysis showed that there was no significant difference in the F4/80+ inflammatory cell area in the two groups (3.7 ± 2% after Ad-sCripto vs 4.6 ± 1% after Ad-Control at day 4; 9.1 ± 4% after Ad-sCripto vs 5.2 ± 3% after Ad-Control at day 8; 5.7 ± 2% after Ad-sCripto vs 6.9 ± 3% after Ad-Control at day 22; n=5 mice/group; P=NS; Figure S4C), thus suggesting that Cripto overexpression does not substantially, contribute to the modulation of the inflammatory process.

### SOLUBLE CRIPTO RESCUES MUSCLE REGENERATION IN MICE WITH CONDITIONAL TARGETED DELETION OF *CRIPTO* IN ADULT SATELLITE CELLS

To evaluate whether soluble Cripto (sCripto) was able to fully recapitulate the

function of endogenous mCripto *in vivo*, we investigated whether sCripto rescued muscle regeneration defects in mice with genetic ablation of *cripto* in adult satellite cells. To this end, *Tg:Pax7-CreERT2::Cripto*$^{loxP/-}$ and control *Cripto*$^{loxP/-}$ mice were injected IP with tamoxifen once a day for 5 days. At day 4, regeneration was triggered in TA muscles by CTX injection, along with local infection of either Ad-sCripto or Ad-Control, and the effect on muscle regeneration was evaluated at day 4 after injury (Figure 5A). We first verified by PCR analysis that *cripto* deletion occurred selectively in skeletal muscles of *Tg:Pax7-CreERT2::Cripto*$^{loxP/-}$ mice (Figure S4E). Accordingly, endogenous Cripto protein levels decreased in muscle tissue of *Tg:Pax7-CreERT2::Cripto*$^{loxP/-}$ compared to control *Cripto*$^{loxP/-}$ mice, as shown by ELISA assay (Figure 5B). As expected, we found that Cripto protein levels strongly increased in Ad-sCripto transduced muscles compared to Ad-Control (Figure 5B). We thus performed morphometric analysis of myofiber size in the different mice groups. As expected, the myofiber CSA was significantly reduced in *Tg:Pax7-CreERT2::Cripto*$^{loxP/-}$ mice compared to *Cripto*$^{loxP/-}$ control. Most remarkably, this reduction was fully rescued by sCripto overexpression in *Tg:Pax7-CreERT2::Cripto*$^{loxP/-}$ mice, and eventually the CSA increased compared to *Cripto*$^{loxP/-}$ control mice, thus providing direct evidence that sCripto was able to fully recapitulate the function of the endogenous mCripto in satellite cells. Furthermore, sCripto overexpression increased myofiber CSA also in control *Cripto*$^{loxP/-}$ mice (Figure 5C-D), thus confirming the positive effect of sCripto in muscle regeneration, and supporting our conclusion.

**CRIPTO PROMOTES MYOGENIC CELL PROLIFERATION**

Results of gain of function and loss of function experiments suggest that Cripto might play a role in regulating satellite cell function and eventually modulate skeletal muscle regeneration. To gain more insight into this issue, we first evaluated whether Cripto would be mitogenic for primary myoblasts in culture. To this end, an enriched population of adult mouse primary muscle precursor cells was isolated and cultured under conditions favoring replication (33), treated with recombinant sCripto, and cell proliferation was measured by BrdU incorporation. Physiological concentrations of recombinant sCripto increased myoblast proliferation in a dose-dependent manner (Figure 6A), and addition of anti-Cripto antibodies nearly completely abolished the mitogenic effects of exogenous Cripto (Figure 6B).

To further investigate Cripto activity on satellite cells in a more physiological context and without bias of selection, we used isolated myofibers in culture, which provide an accessible means to study satellite cells in their native position beneath the basal lamina that surrounds each muscle fiber (26). We first performed immunofluorescence analysis for the proliferation marker Ki67 on freshly isolated myofibers, treated with recombinant sCripto or left untreated as control. In line with results on primary myoblasts, the number of proliferating Ki67+ cells increased in myofibers treated with sCripto by 72 hours compared to control (211 ± 6% after sCripto vs 69 ± 3.7% after control; Figure 6C), thus providing further evidence for a mitogenic activity of Cripto.

Finally, given that Cripto is a GPI-anchored membrane protein in its physiological configuration (34), we also evaluated the effect of membrane Cripto (mCripto). To further assess the paracrine/juxtacrine ability of mCripto, we used single myofibers isolated from *Myf5*$^{nlacZ/+}$ mice plated on feeder layers of mammalian cells, either control or stably expressing mCripto (34), followed by counting the number of βgal+ proliferating primary

myogenic cells. In keeping with our findings, βgal+ cells had almost doubled in the presence of mCripto, compared to control (44 ± 0.58 vs 22 ± 5.78 respectively; n=3 independent experiments; *P=0.0192; Figure 6D).

### CRIPTO MODULATES MYOGENIC CELL DETERMINATION ON ISOLATED MYOFIBERS

To gain further insight into the role of Cripto on satellite cells, we performed a time course immunofluorescence analysis for Pax7 and MyoD on isolated myofibers, treated with recombinant sCripto or left untreated as control. By 48 hours, supplementation of sCripto resulted in a reduced number of quiescent Pax7+/MyoD- cells compared to control (Figure 6E, green bars), thus suggesting that Cripto might promote/accelerate the entry of satellite cells into S phase. Moreover, by 72 hours and up to 96 hours in culture, the number of Pax7-/MyoD+ cells committed to differentiation progressively increased in sCripto-treated myofibers at the expense of Pax7+/MyoD- cells (33 ± 3% for sCripto vs 18 ± 3% of Pax7-/MyoD+ cells for control at 72 hours; *P<0.05; 48 ± 2% for sCripto vs 23 ± 4% for control at 96 hours; **P<0.005; Figure 6E, red bars).

We thus decided to assess whether the duration of Cripto signaling was critical for its biological activity; isolated myofibers were then cultured in the presence of sCripto for 48 hours (0-48 hours), washed to remove Cripto and then cultured for the remaining 48 hours, i.e. up to 96 hours in total. Interestingly, the number of Pax7-/MyoD+ cells increased to the same extent as observed for cells treated with Cripto throughout the culture (43 ± 4% for sCripto vs 23 ± 4% for control after 96 hours; **P<0.005; Figure 6E, red bars), suggesting that treatment of 48 hours is sufficient to induce an effective Cripto response.

Finally, as shown for soluble sCripto (Figure 6E), immunofluorescence analysis of isolated myofibers infected with mCripto–overexpressing lentivirus revealed an increased

number of Pax7-/MyoD+ cells, compared to lenti-Control infected fibers at 72 hours (41.8 ± 2.1% after mCripto vs 25.9 ± 2.3% after control; n=3 experiments; *P<0.01 and **P<0.001; Figure S5A).

Taken together, our data suggest that Cripto plays a dual role, by increasing the proliferation of myogenic cells and by promoting satellite cell progression into the myogenic lineage.

### CRIPTO ANTAGONIZES THE EFFECT OF MYOSTATIN/GDF8 ON SATELLITE CELLS IN ISOLATED MYOFIBERS

Previous findings indicated that Cripto contribute to the modulation of cell proliferation and growth by antagonizing members of the TGFβ superfamily, such as TGFβ itself or Activin (15, 35). Myostatin/GDF8, is a TGFβ family member and a strong inhibitor of muscle growth, and is expressed by quiescent satellite cells (36). To explore the molecular mechanism of Cripto signaling on satellite cells, we investigated whether Cripto may act as an antagonist of Myostatin/GDF8 (GDF8). We therefore first measured the ability of GDF8 to activate Smad2 phosphorylation in the absence or presence of Cripto. To this end, 293 cells were transfected with sCripto expressing plasmid or empty control vector and treated with increasing doses of recombinant GDF8 (Figure 7A). In line with our hypothesis, GDF8–induced Smad2 phosphorylation was inhibited by sCripto, even at the highest concentrations of GDF8 tested (Figure 7A). Moreover, sCripto was able to reduce GDF8–induced Smad2 phosphorylation also in C2C12 myogenic cells (Figure S5B). Remarkably, membrane anchored mCripto retained its ability to antagonize GDF8 signaling (Figure S5C). Furthermore, in agreement with the idea that Cripto/GDF8 may regulate satellite cell myogenic commitment, blocking GDF8 activity by adding anti-GDF8 antibodies to the fibers, increased tendency to differentiation of satellite cells, as indicated

by increased number of Pax7-/MyoD+ cells, at different time points (178 ± 6.0 cells for anti-GDF8 vs 48 ± 2.4 cells for Control at 72hrs, **P=0.005; Figure 7B). Moreover, addition of sCripto to anti-GDF8–treated myofibers did not further increase Pax7-/MyoD+ cell number (211 ± 8.0 cells; **P=0.005; Figure 7B, red bars).

We then investigated whether there was a functional interaction between Cripto and GDF8 signaling pathways on isolated myofibers. As expected, sCripto–treatment resulted in increased number of Pax7-/MyoD+ cells by 72 hours in culture (201 ± 5.5 cells with sCripto vs 49 ± 6.7 cells with control; n=7 independent experiments; **P=0.005; Figure 7B and 7C). We next asked whether Cripto might directly antagonize the effect of GDF8 (R&D; 50-200ng/ml) on satellite cell determination. As expected, GDF8 treatment increased the number of Pax+/MyoD- quiescent and/or self-renewed satellite cells on isolated myofibers, at the expense of MyoD+ cells in a dose-dependent manner (88.67 ± 6.7cells, 121.4 ± 5.9 cells and 168 ± 3.8 cells at 50, 100 and 200 ng/ml respectively; Figure 7D, bars II, V and VIII). On the other hand, addition of anti-GDF8 blocking antibodies blocked the anti-proliferative effect of GDF8 and expansion of the pool of satellite cells committed to myogenic lineage (Figure 7D, bars III, VI and IX). Most interestingly, addition of sCripto (200ng/ml) almost completely reversed the outcome of GDF8 treatment on cell proliferation as well as on Pax7±/MyoD± satellite cell distribution, even at the highest concentration of GDF8 used; i.e. 200ng/ml (Figure 7D, bars IV, VII and X).

Consistent with the idea that Cripto could act as an antagonist of Myostatin/GDF8, we showed that Cripto and Myostatin are expressed in regenerating muscles (Figures S5D and S5E)

All together these data revealed a functional interaction between Cripto and Myostatin/GDF8 signaling pathways to modulate myogenic cell determination.

## DISCUSSION

The capacity of the skeletal muscle regenerative response is primarily due to a resident population of myogenic stem cells, the satellite cells. It is well known that extrinsic and intrinsic signaling pathways modulate the status of the satellite cell pool (37) however, the molecular mechanisms are not yet fully defined.

Here, we demonstrate that Cripto, a critical signal in embryonic development, is re-expressed in adult skeletal muscles that undergo regeneration and that its activity can modulate skeletal muscle regeneration. We show that Cripto is undetectable in quiescent Pax7+/MyoD- satellite cells, but it accumulates in activated satellite cells, being co-expressed with myogenic lineage markers, such as Pax7, Myf5 and MyoD; thus suggesting that Cripto expression occurs concomitantly and/or following activation of satellite cells. Interestingly, Cripto is also expressed in inflammatory cells, during regeneration. Notably, in addition to myogenic cells, inflammatory cells, which are recruited to the damaged area, also provide important contribution to muscle regeneration. Indeed, recent studies have shown that factors expressed during the inflammatory process can influence skeletal muscle regeneration by stimulating satellite cell survival and/or proliferation (38, 39). For example, recent data provided evidence that infiltrating inflammatory cell–derived granulocyte colony-stimulating factor (G-CSF) enhance myoblast proliferation and facilitate skeletal muscle regeneration, thereby underscoring the importance of inflammation-mediated induction of muscle regeneration (39). Conditional Cripto inactivation in adult satellite cells allowed us to unmask the cellular contribution of Cripto *in vivo* and provide novel evidence for a functional role of this protein during muscle regeneration. Notably, although our data do not rule out the possibility that Cripto expressed by infiltrating macrophages would also contribute to this effect, our findings simply indicate that this was not sufficient to compensate for the lack of Cripto in satellite

cells.

In line with these findings, we demonstrate that Cripto modulates the different fates of satellite cells and that it is mitogenic for satellite cell–derived myoblasts. To address this issue, we used isolated myofibers in culture, which allows investigation of effect of exogenous factors on satellite cells in their native positions (26), and found that exposure to either soluble or GPI-anchored Cripto increased the number of Pax7-/MyoD+ committed myogenic cells at the expense of Pax7+/MyoD- cells, suggesting that Cripto promotes/accelerates the entry of satellite cells into S phase and their commitment to differentiation. Moreover, we show that Cripto promotes proliferation both in isolated myofibers and in primary myoblasts in culture. This notion is consistent with previous findings that support a model in which Cripto possesses intrinsic activities as trans-acting factor both in cell culture and *in vivo* (6-8, 31). In line with this idea, soluble Cripto was able to fully rescue the effect on muscle regeneration of the genetic ablation of *cripto* in adult satellite cells. To our knowledge, this represents the first *in vivo* evidence in the mouse that soluble Cripto recapitulates the function of GPI-anchored Cripto.

Several molecules have been described, which regulate stem cell proliferation and/ differentiation and eventually muscle regeneration, including those belonging to the TGFβ superfamily (11). Interestingly, in addition to its obligate role as Nodal/GDF1/GDF3 co-receptor, Cripto can also antagonize signaling by Activins and TGFβ (13-15). GDF8/Myostatin is a member of the TGFβ superfamily that has been implicated in the negative regulation of muscle growth and regeneration (36). Consistent with the idea that Cripto could act as an antagonist of Myostatin/GDF8, we show that Cripto and Myostatin are expressed in regenerating muscles and, most remarkably, that (i) both secreted and membrane anchored-Cripto are able to attenuate Myostatin /Smad2 signaling pathway, (ii) Cripto antagonizes the anti-proliferative effect of Myostatin on isolated myofibers,

promoting myogenic commitment, and similarly, iii) blocking Myostatin activity increases the tendency toward differentiation of satellite cells.

Myostatin is expressed by quiescent satellite cells and has a functional role in repressing satellite cell proliferation and enhancing self-renewal (McCroskery et al 2003). A number of factors have been discovered that antagonize Myostatin activity, such as Follistatin (24), recently suggested to induce muscle hypertrophy through satellite cell proliferation and inhibition of both Myostatin and Activin (40). However, the direct relevance of Myostatin for satellite cells is still debated and controversial models have been proposed regarding which cell types mediate the effects of Myostatin on muscle physiology (41, 42).

Several lines of evidence suggested that the normal function of Myostatin in adult muscle is to maintain satellite cells in a quiescent state, acting as a negative regulator of cell activation and proliferation (36, 43, 44). Moreover, studies in chick and mouse embryos pointed to a context-dependent effect of Myostatin, controlling the balance between proliferation and differentiation on muscle progenitors (45). In contrast, recent data indicate that postnatal muscle hypertrophy generated by the lack of myostatin is largely due to hypertrophy of individual fibers and not to satellite cell activity (46). Indeed, it has been reported that the addition of recombinant Myostatin (100 ng/ml) does not influence satellite cell proliferation *in vitro*. Notably, in that study Myostatin was added to isolated fibers after 48 hours in culture and maintained over the subsequent 24 hours (46). Our protocol differs from this in that both sCripto and/or Myostatin (50-200ng/ml) were added to myofibers immediately after culture, which might explain the apparent discrepancy. We found that in this experimental setting Myostatin is able to inhibit and/or delay the progression of Pax7+/MyoD- quiescent satellite cells towards Pax7+/MyoD+ myogenic/proliferating cells. Interestingly, this effect is reverted by sCripto and also

persists upon removal of Cripto after 48 hours. Although we cannot rule out the possibility that residual Cripto might remain bound to the fibers/cells, thus explaining the long lasting effect of the treatment, previous findings in embryonic stem cells (ESCs) showed that the transient presence of sCripto in the early time window of differentiation (0-48hr) was sufficient to fully rescue the cardiac phenotype of *cripto*$^{-/-}$ ESCs at later time points (31).

In conclusion, we identified Cripto as a novel factor required for efficient repair of skeletal muscles and propose that Cripto regulates satellite cell progression toward the myogenic lineage, at least in part, by counteracting Myostatin activity. Although we cannot rule out the possibility that other signaling pathways might also be involved, our intriguing findings are in line with very recent data, which report that overexpression of Cripto antagonized Myostatin –induced A3 luciferase activity in 293T cells (47). In contrast to these findings, it has been recently proposed that Cripto may also exert a stimulatory role on Myostatin signaling, suggesting that Cripto–mediated Myostatin signaling is dose-dependent (48). Although further experiments will be necessary to elucidate the molecular basis of this newly identified Cripto/Myostatin interaction, our study indicates that this could represent a novel mechanism for the control of satellite cell decisions, necessary for robust skeletal muscle maintenance and repair.

Finally, our findings that Cripto is expressed both in myogenic and inflammatory cells places Cripto within a complex regulatory network which links inflammation and skeletal muscle regeneration, a relationship which remains incompletely understood, and thus opens the way to assess the potential of Cripto as target for the treatment of skeletal muscle injury or disease.

## EXPERIMENTAL PROCEDURES

### SECTION IMMUNOSTAININGS

Muscles were freshly frozen and cut in cryostat sections. Slides were fixed in 4% paraformaldehyde (PFA), permeabilized with 0.5% Triton X-100 (Sigma) and boiled 15 min in sodium-citrate 10mM. Primary antibodies used: anti-Cripto [(6) - 7µg/ml; Santa-Cruz, 1:50; Abcam, 1:150)], anti-Laminin (1:50, AbCam), anti-MyoD (1:20, Dako), F4/80 (1:50; Serotec), Desmin (1:50, ICN). Appropriate fluorophore conjugated secondary antibodies, Alexa Fluor 488 and 594 (Molecular Probes, 1:300) or Dako antibodies –HRP conjiugated and Fluorescein labeled tyramide (PerkinElmer), were used for visualization. Vectashield medium containing 4,6-diamidino-2-phenylindole (DAPI) (Vector Laboratories, Burlingame, CA) was used for mounting. Sections incubated without primary antibodies served as controls. Labeling was visualized by epifluorescent illumination using an Axiovision microscope, and images were acquired on an Axiocam (Zeiss) or Leica (DFC480, DFC350FX) cameras.

### ISOLATION AND GROWTH OF MOUSE PRIMARY MYOBLASTS

Purification of primary myoblast culture was performed as previously described (33, 49). See Supplemental Data for details.

### CELL PROLIFERATION ASSAYS

Myoblasts were cultured at $5x10^4$ cells per well on 96-well microtiter plates in growth medium for few hours and then serum starved overnight in Dulbecco's modified Eagle medium (DMEM) with 0.5% FBS. After washing cells were cultured in DMEM-FBS-0.5% medium containing soluble recombinant mouse Cripto (sCripto; 5, 50, 100, 250, 500 ng/ml,

R&D system and home made production (6), human bFGF (R&D Systems-Minneapolis, MN; 10 ng/ml) or neutralizing antibodies at 4 µg/ml (anti-Cripto, MAB1538, R&D system;). BrdU cell proliferation assay kit (Roche, Indianapolis, IN) was used following manufacturer's instructions. The BrdU incorporation was measured by the absorbance of the samples in an ELISA reader at 370 nm (reference wavelength: approximately 492 nm).

**SINGLE FIBER CULTURE ASSAYS**

Single floating myofibers were prepared from the EDL muscles from 6 weeks-old C57/Bl6 or *Myf5*$^{nlacZ/+}$ mice (27, 50), as described (26, 51). Individual intact myofibers were placed in HS coated round bottom eppendorf tubes and incubated with or without mouse sCripto (R&D system, 200ng/ml) or Myostatin/GDF8 (R&D system, 50, 100 or 200ng/ml) in low activation medium (10% HS, 0.5% CEE in DMEM). Myofibers were treated with sCripto or pre-incubated for 1 hr with either blocking anti-Cripto (MAB1538, R&D system, 4µg/ml) or anti-Myostatin/GDF8 (Neuromics GT15213, 10µg/ml) antibodies prior to Cripto addition.

In the anti-GDF8 time course experiment, myofibers were incubated, during 48, 72 or 96h, with anti-GDF8 (Neuromics GT15213, 10µg/ml) either alone or pre-incubated 1h with GFD8 (200ng/ml). After 48 hrs or 72 hrs of treatment, floating fibers were fixed in 4% PFA, rinsed in PBS and immediately used for immunostaining. Primary antibodies used are: MyoD (1:50, Dako or Santa-Cruz), Pax7 (1:10, DSHB; Zammit et al. 2004), β-Gal (1:350; Biogenesis, Brentwood, NH) and Ki67 (1:250, Abcam; Abou-Khalil et al. 2009).

Alternatively, *Myf5*$^{nlacZ/+}$ myofibers were plated on a feeder layer of mammalian cells expressing membrane-bound Cripto or a mock vector, in 24 multiwell plate in proliferating medium (20% FBS, 10% HS, 1% CEE in DMEM). LacZ staining was performed after 72 hrs to identify activated satellite cells both on the fibers and that have left the fiber.

## MICE AND GENOTYPING

The *Cripto*$^{loxP/-}$ mice were generated by crossing *Cripto*$^{loxP/loxP}$ (8) and *Cripto*$^{+/-}$ (Xu et al., 1999) animals and genotyped by PCR analysis with specific oligos that generate a 197bp (allele [-]) and a 580bp (allele [loxP]) band. The *Tg:Pax7-CreERT2::Cripto*$^{loxP/-}$ mice were generated by crossing *Pax7-CreERT2* and *Cripto*$^{loxP/-}$ animals and genotyped by PCR with primers mapping on *Cre* sequence, generating a 600bp band. The *Cripto* floxed allele (Cripto Del) is detected as a *600-bp* band. Genotyping strategies of Cripto$^{loxP/loxP}$ (8) and Cripto$^{+/-}$ (Xu et al., 1999) have been published. Sequence of primers are shown in Table S2

## MUSCLE INJECTIONS, PREPARATION AND ANALYSIS

Ten µl CTX ($10^{-3}$ M in PBS) or 10 µl CTX ($10^{-3}$ M in PBS) were injected in the tibialis anterior (TA) from 8 weeks old Balbc mice, in the CTX mouse models of more severe or less severe muscle damage, respectively. Following CTX injection, mice were injected intramuscular with Ad-sCripto, generated using *AdEasy™ XL System* (Stratagene), or with Adeno-control (Ad-Control; $4x10^9$ pfu, in a total volume of 25 µl) and muscles were harvested at the indicated time points after damage.

Adult (1 month) Tg:Pax7-CreERT2::CriptoloxP/- and CriptoloxP/- mice were injected IP with tamoxifen (SIGMA-T5648, 60mg/g day) or sesame oil (SIGMA-S3547), as control vehicle, once a day for 5 days. At day 4, CTX (15 µl, 10-5 M in PBS, SIGMA-C9759) was injected into Tibialis anterior (TA) muscle. In the rescue experiment, following CTX injection, mice were injected intramuscularly with either Ad-sCripto or Adeno-control. For morphological and morphometric analysis, muscles were either embedded unfixed in tissue-tek and frozen in isopentane cooled in liquid nitrogen for cryosection or fixed in PFA

and embedded in paraffin. Tissue necrosis was identified by morphological alterations of myofibers, i.e. hypercontraction or loss of sarcolemmal integrity and by the presence of cellular debris in the surrounding interstitial space (52). Regenerated myofibers were identified by the presence of central nuclei, and fibers diameter or cross sectional area were morphometrically analyzed using KS300 image analysis software (Carl Zeiss Inc.) or ImageQuant software (Leica QWin).

**DNA PLASMIDS, CELL CULTURE, AND WESTERN BLOT**

sCripto and mCripto were previously described (6, 34). Briefly, mCripto corresponds to the full-length cripto cDNA, while sCripto corresponds to cripto cDNA with a STOP codon at nucleotide +156.

293T or C2C12 cells were plated on 6-well plates at a density of $2x10^5$. Twenty-four hours after plating cells were tranfected with 4µg of DNA (pCDNA3, pCDNA3-sCripto and pCDNA3-mCripto), using Lypofectamin (Invitrogen). Twenty-four hours after transfection, cells were serum-starved during 8 hrs prior to treatment. Cells were left untreated or treated for 30 min with the indicated doses of Myostatin/GDF8 protein (R&D). Total protein extracts was prepared and analyzed by Western blot as previously described (53). Anti-Phospho-Smad2 (P-Smad2), Smad2 (Cell Signaling Technology), Cripto antibodies (R&D) were used as previously described (31).

**RNA PREPARATION AND RT-PCR**

Total RNAs from TA were isolated using RNeasy mini kit (Qiagen) according to manufacturer's instruction. One microgram of total RNA was used for cDNA synthesis using SuperScript II reverse transcriptase (Life Technologies Inc.) and random hexamers.

qRT-PCR was performed using SYBR Green PCR master mix (EuroClone). Primers listed in Table S1.

### STATISTICAL ANALYSIS

All values are expressed as mean ± standard error of the mean (SEM). To determine significance between two groups, comparisons were done using the unpaired Student t-tests. Analyses of multiple groups were performed using paired Student t-tests using GraphPad Prism version 5.00 for Mac, GraphPad Software, San Diego California USA, www.graphpad.com. $P<0.05$ considered statistically significant.


## Acknowledgments

We thank the Animal House, the Integrated Microscopy and the FACS Facilities of IGB-CNR for technical assistance, Sabine Wyns for helping in generating Cripto-Adenovirus, and Ann Carton for technical support. This work has benefited from research funding from the European Community's Seventh Framework Programme in the project ENDOSTEM (Activation of vasculature associated stem cells and muscle stem cells for the repair and maintenance of muscle tissue Grant agreement number 241440) to GM and SB; Telethon (GGP08120), AIRC, Ministero Istruzione Università Ricerca [Medical Research in Italy RBNE08HM7T_003] to GM and Association Française contre les Myopathies (AFM) to GM, PC and PL. PL was supported by an EMBO Long-term Fellowship.

## REFERENCES


1. Beachy PA, Karhadkar SS, & Berman DM (2004) Tissue repair and stem cell renewal in carcinogenesis. (Translated from eng) *Nature* 432(7015):324-331 (in eng).
2. Shen MM & Schier AF (2000) The EGF-CFC gene family in vertebrate development. (Translated from eng) *Trends Genet* 16(7):303-309 (in eng).
3. Assou S*, et al.* (2007) A meta-analysis of human embryonic stem cells transcriptome integrated into a web-based expression atlas. (Translated from eng) *Stem Cells* 25(4):961-973 (in eng).
4. Minchiotti G (2005) Nodal-dependant Cripto signaling in ES cells: from stem cells to tumor biology. (Translated from eng) *Oncogene* 24(37):5668-5675 (in eng).
5. Miharada K*, et al.* (2011) Cripto regulates hematopoietic stem cells as a hypoxic-niche-related factor through cell surface receptor GRP78. (Translated from eng) *Cell Stem Cell* 9(4):330-344 (in eng).
6. Minchiotti G*, et al.* (2001) Structure-function analysis of the EGF-CFC family member Cripto identifies residues essential for nodal signalling. (Translated from eng) *Development* 128(22):4501-4510 (in eng).
7. Bianco C*, et al.* (2002) Cripto-1 activates nodal- and ALK4-dependent and -independent signaling pathways in mammary epithelial Cells. (Translated from eng) *Mol Cell Biol* 22(8):2586-2597 (in eng).
8. Chu J*, et al.* (2005) Non-cell-autonomous role for Cripto in axial midline formation during vertebrate embryogenesis. (Translated from eng) *Development* 132(24):5539-5551 (in eng).
9. Reissmann E*, et al.* (2001) The orphan receptor ALK7 and the Activin receptor ALK4 mediate signaling by Nodal proteins during vertebrate development. (Translated from eng) *Genes Dev* 15(15):2010-2022 (in eng).
10. Cheng SK, Olale F, Bennett JT, Brivanlou AH, & Schier AF (2003) EGF-CFC proteins are essential coreceptors for the TGF-beta signals Vg1 and GDF1. (Translated from eng) *Genes Dev* 17(1):31-36 (in eng).
11. Shi X & Garry DJ (2006) Muscle stem cells in development, regeneration, and disease. (Translated from eng) *Genes Dev* 20(13):1692-1708 (in eng).
12. Massague J & Chen YG (2000) Controlling TGF-beta signaling. (Translated from eng) *Genes Dev* 14(6):627-644 (in eng).
13. Adkins HB*, et al.* (2003) Antibody blockade of the Cripto CFC domain suppresses tumor cell growth in vivo. (Translated from eng) *J Clin Invest* 112(4):575-587 (in eng).
14. Gray PC, Harrison CA, & Vale W (2003) Cripto forms a complex with activin and type II activin receptors and can block activin signaling. (Translated from eng) *Proc Natl Acad Sci U S A* 100(9):5193-5198 (in eng).
15. Gray PC, Shani G, Aung K, Kelber J, & Vale W (2006) Cripto binds transforming growth factor beta (TGF-beta) and inhibits TGF-beta signaling. (Translated from eng) *Mol Cell Biol* 26(24):9268-9278 (in eng).
16. Adamson ED, Minchiotti G, & Salomon DS (2002) Cripto: a tumor growth factor and more. (Translated from eng) *J Cell Physiol* 190(3):267-278 (in eng).
17. Strizzi L, Bianco C, Normanno N, & Salomon D (2005) Cripto-1: a multifunctional modulator during embryogenesis and oncogenesis. (Translated from eng) *Oncogene* 24(37):5731-5741 (in eng).
18. Charge SB & Rudnicki MA (2004) Cellular and molecular regulation of muscle regeneration. (Translated from eng) *Physiol Rev* 84(1):209-238 (in eng).
19. Seale P*, et al.* (2000) Pax7 is required for the specification of myogenic satellite cells. (Translated from eng) *Cell* 102(6):777-786 (in eng).

20. Tedesco FS, *et al.* (2011) Stem cell-mediated transfer of a human artificial chromosome ameliorates muscular dystrophy. (Translated from eng) *Sci Transl Med* 3(96):96ra78 (in eng).
21. Tajbakhsh S (2005) Skeletal muscle stem and progenitor cells: reconciling genetics and lineage. (Translated from eng) *Exp Cell Res* 306(2):364-372 (in eng).
22. Tatsumi R, Anderson JE, Nevoret CJ, Halevy O, & Allen RE (1998) HGF/SF is present in normal adult skeletal muscle and is capable of activating satellite cells. (Translated from eng) *Dev Biol* 194(1):114-128 (in eng).
23. Musaro A & Rosenthal N (1999) Maturation of the myogenic program is induced by postmitotic expression of insulin-like growth factor I. (Translated from eng) *Mol Cell Biol* 19(4):3115-3124 (in eng).
24. Lee SJ & McPherron AC (2001) Regulation of myostatin activity and muscle growth. (Translated from eng) *Proc Natl Acad Sci U S A* 98(16):9306-9311 (in eng).
25. Otto A, *et al.* (2008) Canonical Wnt signalling induces satellite-cell proliferation during adult skeletal muscle regeneration. (Translated from eng) *J Cell Sci* 121(Pt 17):2939-2950 (in eng).
26. Zammit PS, *et al.* (2004) Muscle satellite cells adopt divergent fates: a mechanism for self-renewal? (Translated from eng) *J Cell Biol* 166(3):347-357 (in eng).
27. Beauchamp JR, *et al.* (2000) Expression of CD34 and Myf5 defines the majority of quiescent adult skeletal muscle satellite cells. (Translated from eng) *J Cell Biol* 151(6):1221-1234 (in eng).
28. Tajbakhsh S, Rocancourt D, & Buckingham M (1996) Muscle progenitor cells failing to respond to positional cues adopt non-myogenic fates in myf-5 null mice. (Translated from eng) *Nature* 384(6606):266-270 (in eng).
29. Ding J, *et al.* (1998) Cripto is required for correct orientation of the anterior-posterior axis in the mouse embryo. (Translated from eng) *Nature* 395(6703):702-707 (in eng).
30. Mourikis P, *et al.* (2011) A Critical Requirement for Notch Signaling in Maintenance of the Quiescent Skeletal Muscle Stem Cell State. (Translated from Eng) *Stem Cells* (in Eng).
31. Parisi S, *et al.* (2003) Nodal-dependent Cripto signaling promotes cardiomyogenesis and redirects the neural fate of embryonic stem cells. (Translated from eng) *J Cell Biol* 163(2):303-314 (in eng).
32. Arsic N, *et al.* (2003) Induction of functional neovascularization by combined VEGF and angiopoietin-1 gene transfer using AAV vectors. (Translated from eng) *Mol Ther* 7(4):450-459 (in eng).
33. Qu Z, *et al.* (1998) Development of approaches to improve cell survival in myoblast transfer therapy. (Translated from eng) *J Cell Biol* 142(5):1257-1267 (in eng).
34. Minchiotti G, *et al.* (2000) Membrane-anchorage of Cripto protein by glycosylphosphatidylinositol and its distribution during early mouse development. (Translated from eng) *Mech Dev* 90(2):133-142 (in eng).
35. Shen MM (2003) Decrypting the role of Cripto in tumorigenesis. (Translated from eng) *J Clin Invest* 112(4):500-502 (in eng).
36. Thomas M, *et al.* (2000) Myostatin, a negative regulator of muscle growth, functions by inhibiting myoblast proliferation. (Translated from eng) *J Biol Chem* 275(51):40235-40243 (in eng).
37. Jang YC, Sinha M, Cerletti M, Dall'osso C, & Wagers AJ (2011) Skeletal Muscle Stem Cells: Effects of Aging and Metabolism on Muscle Regenerative Function. (Translated from Eng) *Cold Spring Harb Symp Quant Biol* (in Eng).

38. Chazaud B, *et al.* (2003) Satellite cells attract monocytes and use macrophages as a support to escape apoptosis and enhance muscle growth. (Translated from eng) *J Cell Biol* 163(5):1133-1143 (in eng).
39. Hara M, *et al.* (2011) G-CSF influences mouse skeletal muscle development and regeneration by stimulating myoblast proliferation. (Translated from Eng) *J Exp Med* (in Eng).
40. Gilson H, *et al.* (2009) Follistatin induces muscle hypertrophy through satellite cell proliferation and inhibition of both myostatin and activin. (Translated from eng) *Am J Physiol Endocrinol Metab* 297(1):E157-164 (in eng).
41. Cassano M, *et al.* (2009) Cellular mechanisms and local progenitor activation to regulate skeletal muscle mass. (Translated from eng) *J Muscle Res Cell Motil* 30(7-8):243-253 (in eng).
42. Bentzinger CF, von Maltzahn J, & Rudnicki MA (2010) Extrinsic regulation of satellite cell specification. (Translated from eng) *Stem Cell Res Ther* 1(3):27 (in eng).
43. Joulia D, *et al.* (2003) Mechanisms involved in the inhibition of myoblast proliferation and differentiation by myostatin. (Translated from eng) *Exp Cell Res* 286(2):263-275 (in eng).
44. Amthor H, Otto A, Macharia R, McKinnell I, & Patel K (2006) Myostatin imposes reversible quiescence on embryonic muscle precursors. (Translated from eng) *Dev Dyn* 235(3):672-680 (in eng).
45. Manceau M, *et al.* (2008) Myostatin promotes the terminal differentiation of embryonic muscle progenitors. (Translated from eng) *Genes Dev* 22(5):668-681 (in eng).
46. Amthor H, *et al.* (2009) Muscle hypertrophy driven by myostatin blockade does not require stem/precursor-cell activity. (Translated from eng) *Proc Natl Acad Sci U S A* 106(18):7479-7484 (in eng).
47. Ciarmela P, *et al.* (2011) Activin-A and myostatin response and steroid regulation in human myometrium: disruption of their signalling in uterine fibroid. (Translated from eng) *J Clin Endocrinol Metab* 96(3):755-765 (in eng).
48. Kemaladewi DU, *et al.* (2011) Cell-type specific regulation of myostatin signaling. (Translated from Eng) *FASEB J* (in Eng).
49. Rando TA & Blau HM (1994) Primary mouse myoblast purification, characterization, and transplantation for cell-mediated gene therapy. (Translated from eng) *J Cell Biol* 125(6):1275-1287 (in eng).
50. Montarras D, *et al.* (2005) Direct isolation of satellite cells for skeletal muscle regeneration. (Translated from eng) *Science* 309(5743):2064-2067 (in eng).
51. Rosenblatt JD, Lunt AI, Parry DJ, & Partridge TA (1995) Culturing satellite cells from living single muscle fiber explants. (Translated from eng) *In Vitro Cell Dev Biol Anim* 31(10):773-779 (in eng).
52. Ferreira R, *et al.* (2009) Proteolysis activation and proteome alterations in murine skeletal muscle submitted to 1 week of hindlimb suspension. (Translated from eng) *Eur J Appl Physiol* 107(5):553-563 (in eng).
53. Kelber JA, Shani G, Booker EC, Vale WW, & Gray PC (2008) Cripto is a noncompetitive activin antagonist that forms analogous signaling complexes with activin and nodal. (Translated from eng) *J Biol Chem* 283(8):4490-4500 (in eng).

## Figure Legends

**Figure 1. Cripto is expressed during skeletal muscle regeneration.**

(A-F) Double immunofluorescence with antibodies anti -Laminin (green) and -Cripto (red) in uninjured TA muscle (A-C) and in CTX-injured TA muscles during regeneration (D-F), showing Cripto expression in regenerating fibers. (G-L) Regenerating muscle sections stained with anti -Cripto (red) and -MyoD or F4/80 (green) antibodies. Co-localization of Cripto and MyoD (green) or F4/80 (green) indicates Cripto expression in myogenic cells (G-I; white arrows) and inflammatory cells (J-L; yellow arrowheads), respectively. Nuclei are stained in blue with DAPI. Scale bars=50 μm. See also Figure S1.

**Figure 2**. **Cripto is expressed in activated/proliferating satellite cells.**

(A-O) Cripto staining with Pax7 and MyoD on teased myofibers isolated from C57BL/6 mice, at different time points in culture: 0 (A-E, T0), 24 (F-J, T24) and 48 hrs (K-O, T48). The Cripto staining images are superimposed on a phase-contrast image (E, J, and O). (A'-O') Insets are higher magnifications of myofibers. Scale bars= 25 μm, 50 μm. See also Figure S2.

**Figure 3. Conditional targeted deletion of *cripto* in satellite cells impairs muscle regeneration after acute muscle damage.**

(A) Schematic representation of conditional loss of function of *Cripto* using *Tg:Pax7-CreERT2::Cripto*$^{loxP/-}$ mice. Tamoxifen or control vehicle were injected IP in adult mice (1 month) once a day for five days. At day 4, regeneration was triggered by CTX injection in TA muscle of both groups, and analysis performed at the indicated time points (day 4 and day 15). (B) PCR analysis showing tamoxifen-induced deletion of *Cripto* floxed allele only in uninjured contralateral TA muscle (left panel) but not in bone marrow (right panel),

isolated at day 15. Genomic DNA isolated from uninjured TA muscles and bone marrow of tamoxifen-treated *Cripto*$^{loxP/loxP}$ CAG-*Cre*ERT2 mice, was used as positive controls (C+). (C) ELISA -based assay of Cripto protein levels in muscle tissue of *Tg:Pax7-CreERT2::Cripto*$^{loxP/-}$ mice treated with either sesam-oil as control, or tamoxifen at day 4 after injury (18.1±0.3 pg/mg control vs 11.05 ± 1.4 pg/mg tamoxifen). Values are mean ± SEM, 3 mice/group, *P=0.04. (D) Representative H&E-stained sections of CTX–treated muscles at indicated time points. Scale bars = 50 μm. (E-F) Cross sectional area (CSA) analysis of regenerated fibers at day 4 (E) and at day 15 (F) showing smaller myofibers in tamoxifen treated mice vs control mice at both time points. See also Table S2.

**Figure 4. Cripto overexpression accelerates muscle regeneration after acute muscle damage.**

(A) Representative pictures from H&E staining of CTX-treated muscles at indicated days after injury, injected with either Ad-Control or Ad-sCripto. Scale bars=100 μm. (B-C) Cripto overexpression induces a faster regeneration as by fiber types repartition. Centrally nucleated myofibers increased in Ad-sCripto vs Ad-Control (B); necrotic fibers area was reduced (C). Results are expressed as percentage of total section area at each time point. Values are mean ± SEM, 5 mice/group, **P<0.005. (D) qRT -PCR analysis of nMyHC expression. Values are mean ± SEM, 5 mice/time point, **P<0.005. (E, F) Cross Sectional Area (CSA) analysis of centrally nucleated fibers at day 8 (E) and day 22 (F) shows increased percentage of large fibers in Ad-sCripto vs control mice, indicating hypertrophy of muscle fibers. See also Figures S3, S4 and Table S1.

**Figure 5. sCripto rescues muscle regeneration in a mouse model of conditional targeted deletion of *cripto* in adult satellite cells**

(A) Schematic representation of conditional loss of function of *cripto* in adult satellite cells, along with adenoviral -mediated sCripto overexpression, in *Tg:Pax7-CreERT2::Cripto*$^{loxP/-}$ and *Cripto*$^{loxP/-}$ mice. B) ELISA assay of Cripto protein levels in muscle tissue at day 4 after injury. Average Cripto levels are plotted for each group/condition. Endogenous Cripto protein was significantly reduced upon targeted deletion of *cripto* in *Tg:Pax7-CreERT2::Cripto*$^{loxP/-}$ compared to *Cripto*$^{loxP/-}$ control, both infected with Ad-Control (26 ± 6.5 pg/mg *Cripto*$^{loxP/-}$ vs 11.8 ±1.8 pg/mg *Tg:Pax7-CreERT2::Cripto*$^{loxP/-}$; *P=0.05). Cripto levels increased (≈1ng/mg) in Ad-sCripto infected mice. Values are mean ± SEM, n=3 mice/group. (C) Representative H&E staining of TA muscle sections from each group. Scale bars = 50 μm. (D) Myofiber CSA distribution and average were reduced in Ad-Control treated *Tg:Pax7-CreERT2::Cripto*$^{loxP/-}$ mice (pink line and bar) compared to *Cripto*$^{loxP/-}$ (green line and bar), and increased upon sCripto overexpression (blu line and bar). Myofiber CSA distribution and average increased in control *Cripto*$^{loxP/-}$ mice overexpressing sCripto (orange line and bar) compared to Ad-Control (green line and bar). Values are mean ± SEM, n=3 mice/group. *P=0.02; **P<0.004. See also Figures S4.

**Figure6. Cripto promotes myoblast proliferation and modulates myogenic cell determination**

(A-B) sCripto induces primary myoblast proliferation in a dose-dependent manner. Cells were cultured during 48h in growth medium (GM curve) or in DMEM-FBS-0.5% medium containing soluble recombinant mouse Cripto protein: commercially available (R&D) and Home-Made production (HM) (6-8). Activity was expressed as fold change over Control/BM, (Basal Medium, 0.5% FBS containing medium). (B). Addition of anti-Cripto

antibodies (R&D), abolished the pro-proliferative effect of sCripto. Activity was expressed as fold change over Control (0.5% FBS containing medium). bFGF was used as positive control, n= 7 independent experiments, **P=0.05. (C) Isolated myofibers treated with sCripto (200ng/ml) for 72hrs show increased number of Ki67+proliferating cells compared to control (n=3 experiments; **P<0.001). (D) Myofibers derived from *Myf5*$^{nlacZ}$ mice plated on a feeder layer of cells stably overexpressing GPI-anchored Cripto (mCripto) show increased number of nlacZ+ myoblasts after 72 hrs in culture, compared to control (n=3 independent experiments; P=0.0192 vs control). (E) Effect of sCripto on Pax7±/MyoD± cell distribution on isolated myofibers. Double staining of fibers cultured for 48, 72 and 96 hrs either alone or in the presence of sCripto. In the presence of sCripto, Pax7+/MyoD- cells (green bar) were absent by 48 hrs. Pax7-/MyoD+ cells (red bar) progressively increased. The percentage of Pax7-/MyoD+ cells did not change significantly in myofibers treated with sCripto for 0-48hrs, compared to control 0-96hrs (n=3 independent experiments, *P<0.05, **P<0.005). Values are mean ± SEM. See also Figure S5.

**Figure 7. Cripto antagonizes Myostatin/GDF8 signaling and counteracts its anti-proliferative effect on satellite cells**

(A) sCripto overexpression reduces Myostatin/GDF8 -induced Smad2 phosphorylation. Total lysates of 293T cells, transfected with empty- or sCripto-vector and treated with increasing doses of Myostatin/GDF8 (R&D), were subjected to Western blot analysis using anti -P-Smad2, -Smad2 or -Cripto antibodies. (B-D) Cripto/GDF8 signaling interaction expanded the pool of satellite cells committed to myogenic lineage. (B) Double staining of fibers cultured for 48, 72 and 96 hrs either alone or in the presence of anti -GDF8 antibodies, and +/- GDF8 protein (left panel); or cultured for 72 hrs with sCripto and anti-GDF8 or anti-Cripto antibodies, either alone or in combination (right panel). The number of

Pax7-/MyoD+ committed cells (red bar) increases in fibers treated with anti -GDF8 antibodies at all time points, and the effect is antagonized by GDF8 (left panel). Similarly, Pax7-/MyoD+ cells (red bar) increases in fibers treated with sCripto, and do not further increase in the presence of anti-GDF8, at 72hrs (n=3 independent experiments, *P<0.05 and **P<0.005 compared to control; right panel). Values are mean ± SEM. (C) Representative pictures from single fibers treated with sCripto ± 1 hr of anti-GDF8 antibodies pre-treatment and stained for Pax7 (green) and MyoD (red). Scale bars=50 μm. (D) Functional titration of GDF8 activity on isolated fibers at 72 hrs. GDF8 increases the number of Pax7+/MyoD- quiescent/self-renewed cells in a dose-dependent manner (50-200 ng/ml; green bars III, VI, IX) compared to control. Fibers pre-treatment with either anti-GDF8 blocking antibodies (bars IV, VII, X) or sCripto (bars V, VIII, XI) blocks the anti-proliferative effect of GDF8; n= 3 independent experiments, *P<0.05 and **P<0.005. Values are mean ± SEM. See also Figure S5.

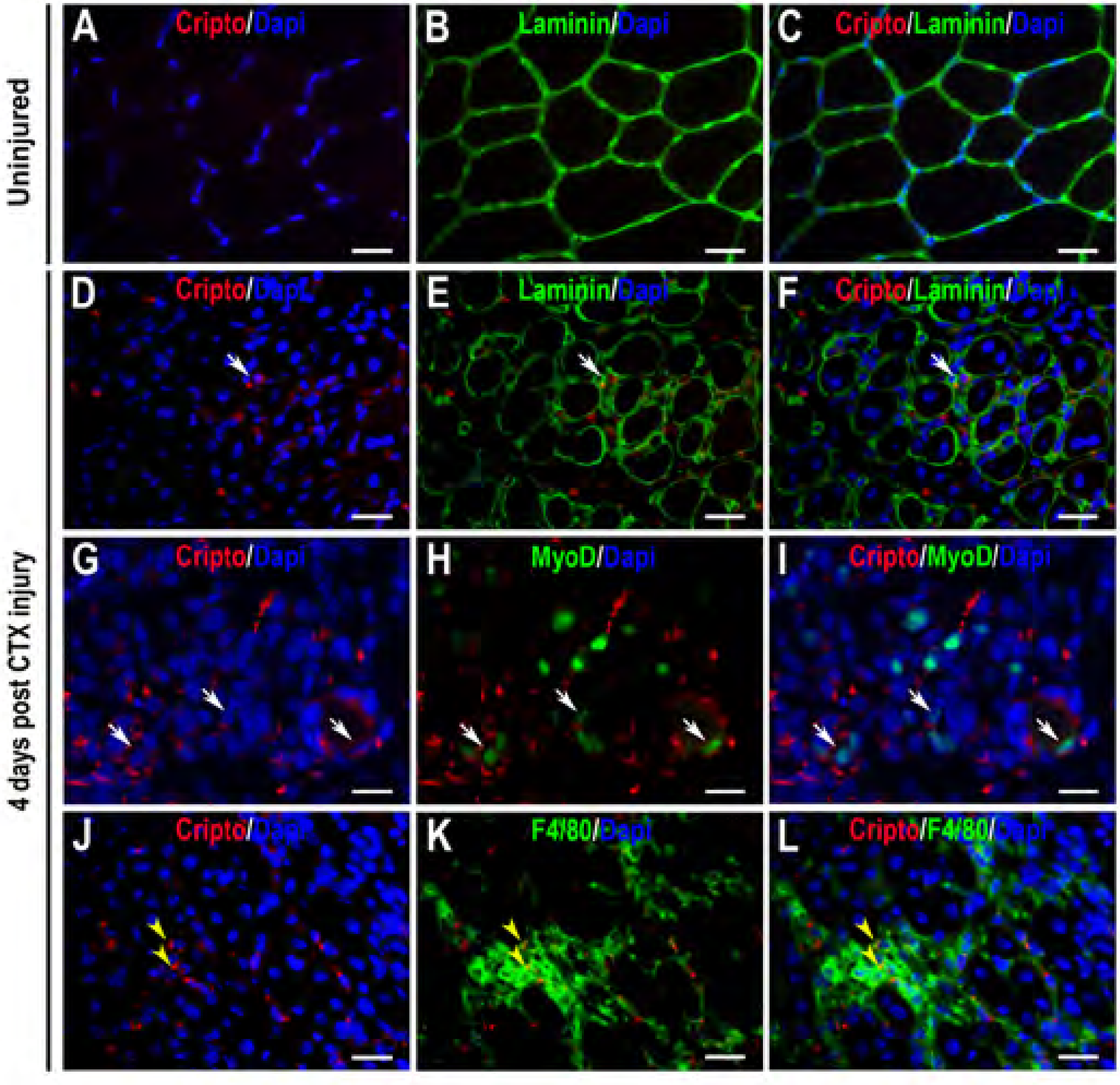
Uninjured
4 days post CTX injury
A
Cripto/Dapi
B
Laminin/Dapi
C
Cripto/Laminin/Dapi
D
Cripto/Dapi
E
Laminin/Dapi
F
Cripto/Laminin/Dapi
G
Cripto/Dapi
H
MyoD/Dapi
I
Cripto/MyoD/Dapi
J
Cripto/Dapi
K
F4/80/Dapi
L
Cripto/F4/80/Dapi

Figure 1

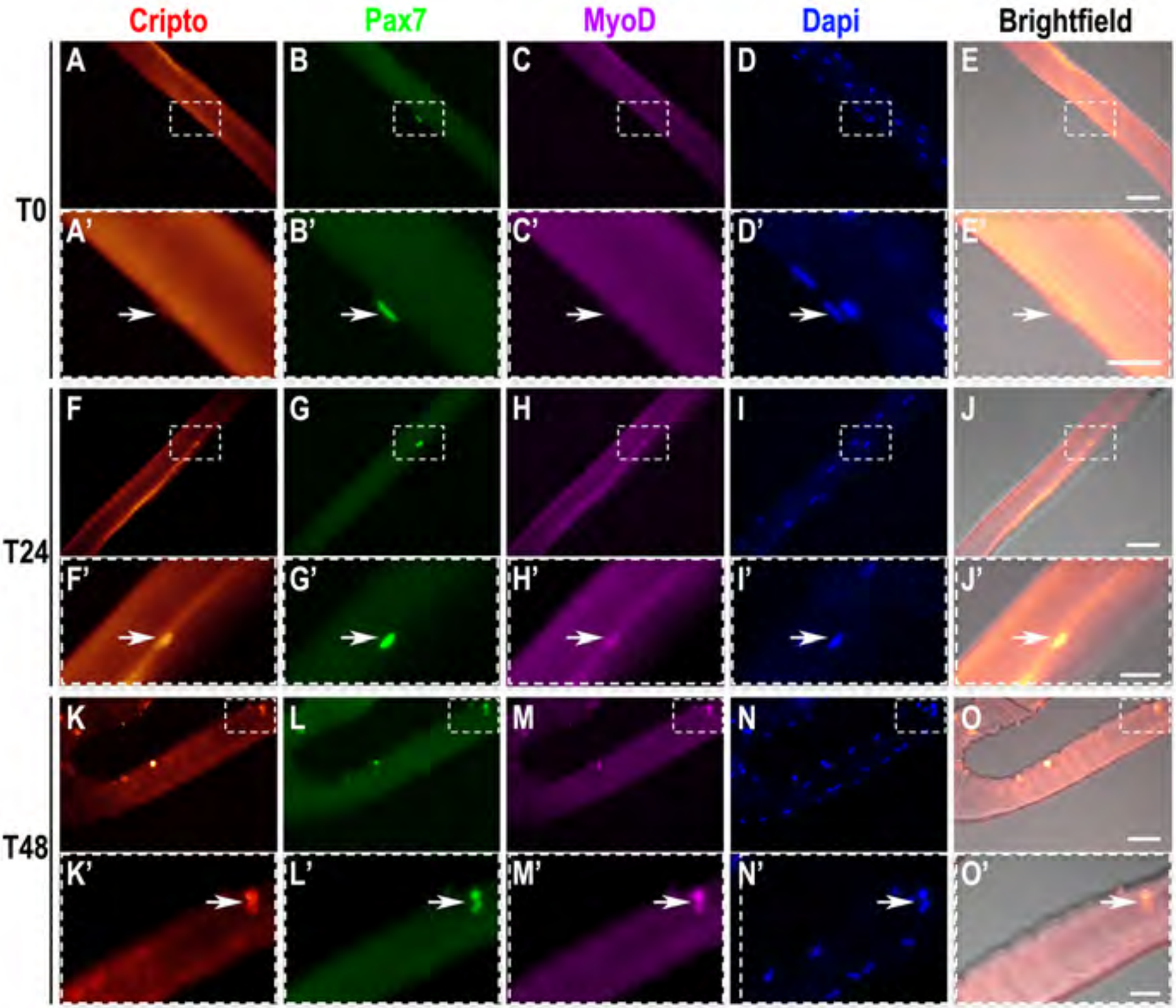
Cripto
Pax7
MyoD
Dapi
Brightfield
T0
T24
T48
A
B
C
D
E
A'
B'
C'
D'
E'
F
G
H
I
J
F'
G'
H'
I'
J'
K
L
M
N
O
K'
L'
M'
N'
O'

Figure 2

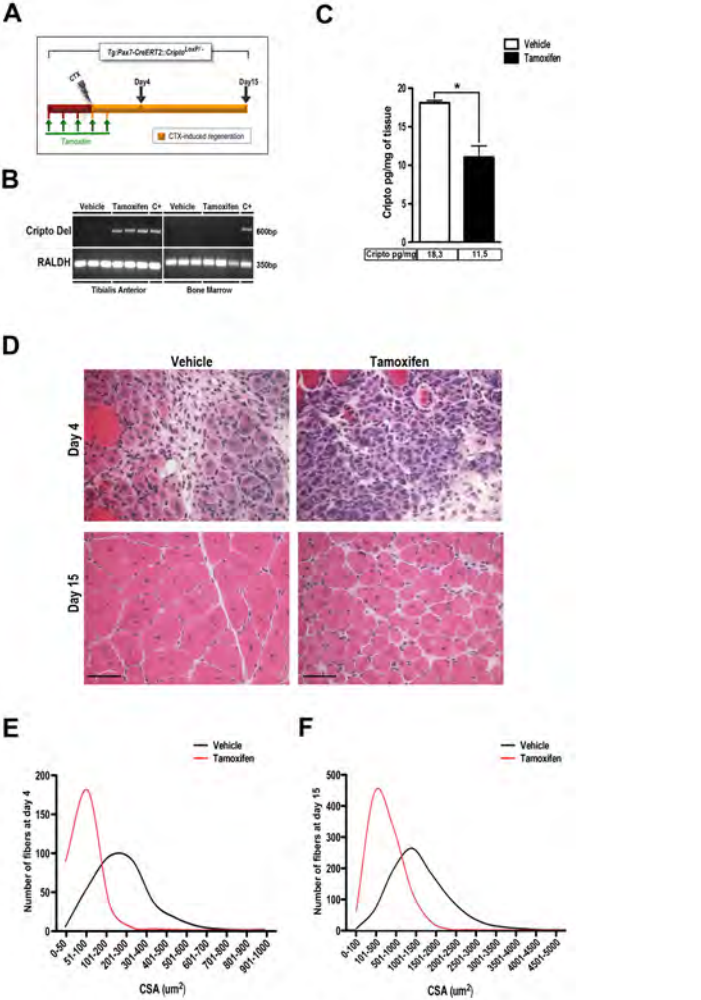
A
Tg:Pax7-CreERT2::Cripto^LoxP/-
CTX
Day4
Day15
Tamoxifen
CTX-induced regeneration
B
Vehicle
Tamoxifen
C+
Vehicle
Tamoxifen
C+
Cripto Del
RALDH
600bp
350bp
Tibialis Anterior
Bone Marrow
C
Vehicle
Tamoxifen
Cripto pg/mg of tissue
*
Cripto pg/mg
18,3
11,5
D
Vehicle
Tamoxifen
Day 4
Day 15
E
Vehicle
Tamoxifen
Number of fibers at day 4
CSA (um²)
F
Vehicle
Tamoxifen
Number of fibers at day 15
CSA (um²)

**Figure 3**

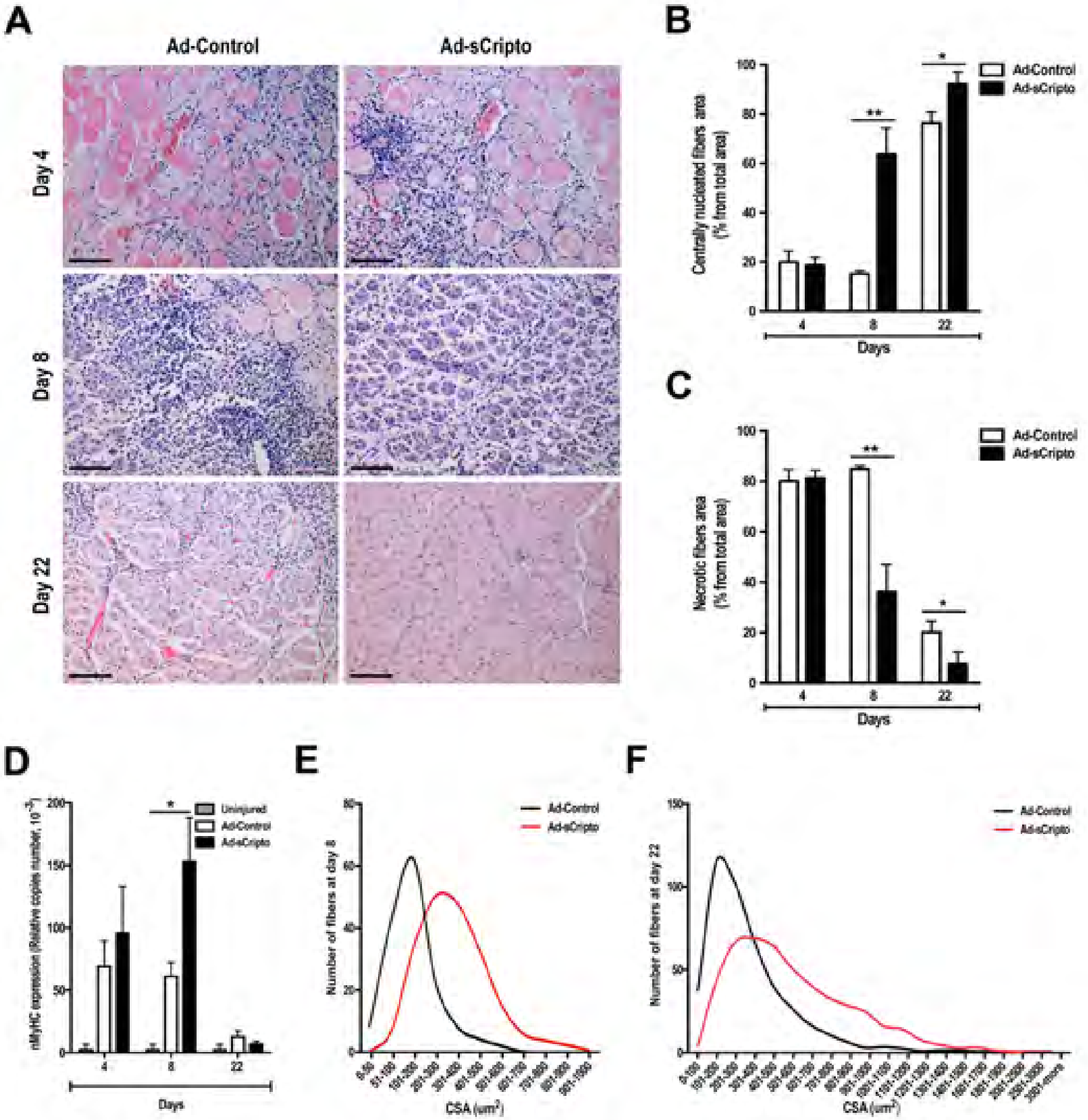
A
Ad-Control
Ad-sCripto
Day 4
Day 8
Day 22
B
Centrally nucleated fibers area (% from total area)
AdControl
Ad-sCripto
Days
C
Necrotic fibers area (% from total area)
Ad-Control
Ad-sCripto
Days
D
nMyHC expression (Relative copies number, 10^-3)
Uninjured
Ad-Control
Ad-sCripto
Days
E
Number of fibers at day 8
Ad-Control
Ad-sCripto
CSA (um²)
F
Number of fibers at day 22
Ad-Control
Ad-sCripto
CSA (um²)

Figure 4

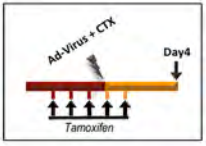
A
Ad-Virus + CTX
Day4
Tamoxifen

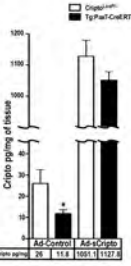
B
Cripto pg/mg of tissue
Ad-Control
Ad-sCripto
Cripto pg/mg
25
11.8
1051.1
1127.8

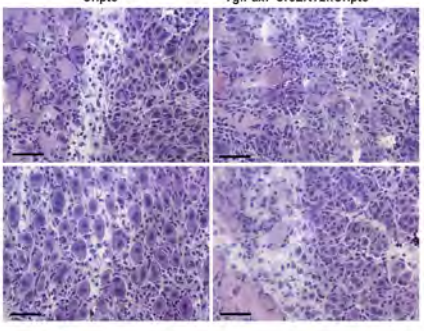
C
Ad-Control
Ad-sCripto

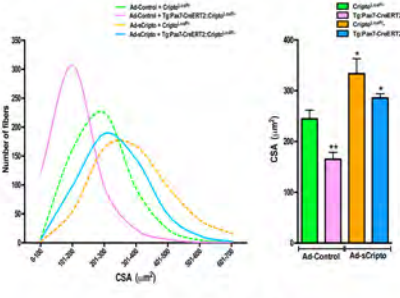
D
Number of fibers
CSA (um²)
Ad-Control
Ad-sCripto

Figure 5

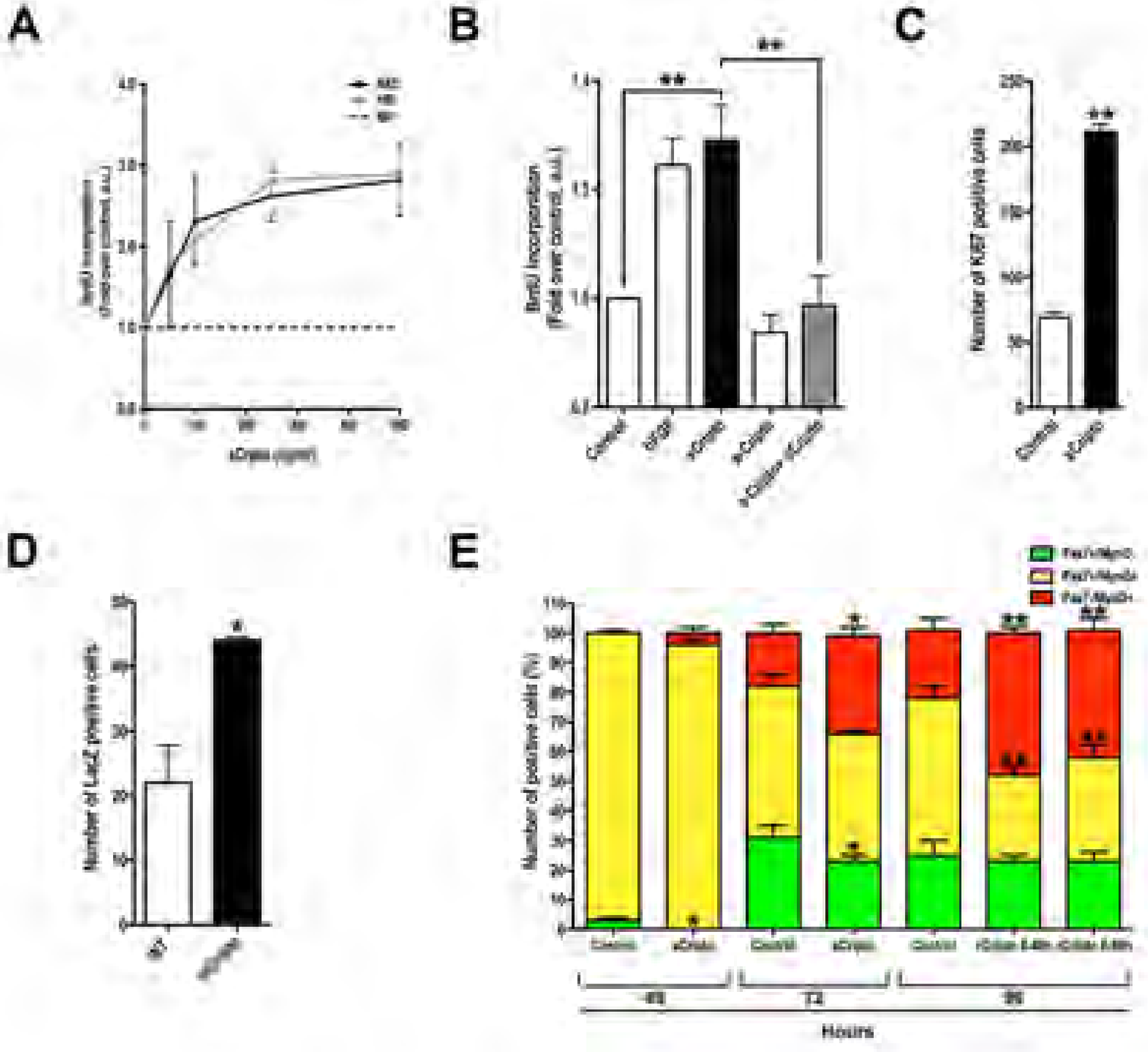


Figure 6

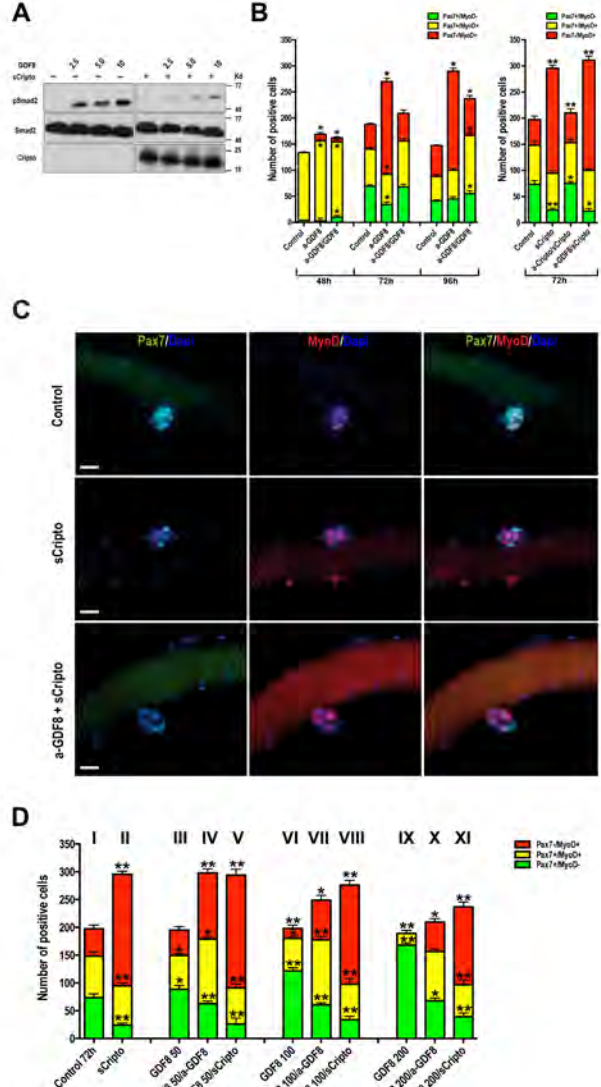
A
GDF8
sCripto
pSmad2
Smad2
Cripto
B
Pax7+/MyoD-
Pax7+/MyoD+
Pax7-/MyoD+
Number of positive cells
Control
a-GDF8
a-GDF8/sCripto
48h
72h
96h
sCripto
a-Cripto/sCripto
C
Pax7/Dapi
MyoD/Dapi
Pax7/MyoD/Dapi
Control
sCripto
a-GDF8 + sCripto
D
I
II
III
IV
V
VI
VII
VIII
IX
X
XI
Control 72h
sCripto
GDF8 50
GDF8 50/a-GDF8
GDF8 50/sCripto
GDF8 100
GDF8 100/a-GDF8
GDF8 100/sCripto
GDF8 200
GDF8 200/a-GDF8
GDF8 200/sCripto

Figure 7

## SUPPLEMENTAL EXPERIMENTAL PROCEDURES

### CELL ISOLATION, TREATMENTS AND FACS ANALYSIS

Briefly forelimbs and hindlimbs were removed from neonatal mice and dissociated by enzymatic digestion; 2 ml dispase (grade II, 2.4 U/ml, Roche) and collagenase B (1%; Roche), supplemented with $CaCl_2$ to a final concentration of 2.5 mM per mg of tissue. Myoblasts were purified and grown in DMEM-Glutamax-I (Invitrogen) supplemented with 20% fetal bovine serum (FBS), 10% horse serum (HS), 1% chick embryo extract (CEE), 1% penicillin–streptomycin, 1% Insulin-Transferin-Selenium X, 10 ng/ml bFGF, 5 ng/ml IGF-I (Invitrogen, Carlsbad, CA).

TA muscles were digested as described above, and unfixed cells were treated with anti-Cripto APC-conjugated (R&D systems) and anti-F4/80 FITC-conjugated (BD Biosciences) antibodies along with the appropriate mouse IgG isotype control. Determination of cell surface expression of Cripto and F4/80 antigens was performed by cytofluorimetric analysis assay using the FACSARIA cell-sorting system and analyzed by the DIVA software (BD Biosciences).

### IMMUNOHISTOCHEMISTRY

Muscles sections were treated as mentioned in experimental procedures for immunofluorescence, then incubated overnight with primary anti-Cripto (1) antibodies (7 µg/ml), followed by incubation with secondary antibodies Goat anti-rabbit HRP -conjugated (1:300; Dako Cytomation) or rat anti-mouse F4/80 antibody (1/50, Serotec) followed by Rabbit anti-rat biotinylated (1:300; Dako Cytomation), streptavidin HRP –conjugated (1/100; Perkin Elmer). Slides were incubated with Betazoid DAB Chromogen kit (Biocare Medical) following

manufacturer's instructions and nuclei were labeled with ematoxilin (Dako) and mounted with Aquatex mounting agent (Merck).

### MACROPHAGES QUANTITATION IN REGENERATING MUSCLES

The number of infiltrated cells was counted in all the fields in regeneration area using ImageQuant software (Leica QWin) and is expressed as the mean number ± SEM per square millimeter.

### ELISA ASSAY

96 wells plates were coated with 0.5ng/ml of home made antiCripto antibodies (2) in PBS (pH 7.5) overnight at 4°C and were washed three times with PBS-Tween. Unbinding sites were blocked with PBS-BSA 1% (180ul/well) for 2h RT. After washing three times, the mouse sera (100µl) or proteic muscles extract (300µg) were added and incubated overnight at 4°C. The plates were incubated with 1µg/ml of anti-Cripto biotinilated antibodies (R&D) in PBE-T for 1 hr at 37°C, then 1 hr at RT. Finally, the plates were incubated for 1hr at RT with avidin/streptavidin complex conjugated with horse-radish peroxidase (Vectastain elite, ABC kit). The plates were then developed with OPD (o-phenylenediamineperoxidase substrate, SIGMA) and the absorbance was read at 490 nm on a Benchmark microplate reader.

### MOUSE MODELS OF LESS SEVERE MUSCLE DAMAGE

For the CTX model, muscle damage was induced as previously described (Experimental Procedures) by injection of 10µl of cardiotoxin ($10^{-5}$ M in PBS; Latoxan) in the tibialis anterior (TA) from 8 weeks old Balbc mice.

Limb ischemia was induced by unilateral right ligation of the femoral artery and vein, distal

from the branching site of the caudal femoral artery and of the cutaneous vessels branching from the caudal femoral artery, sparing the femoral nerve.

### REVERSE TRANSCRIPTION PCR- ADD Q-RT

Total RNA from the cells and/or skeletal muscles was extracted with TRIZOL Kit (Life Technologies) according to the manufacturer's instructions. Muscle tissue was homogenized with TissueLyser (QIAGEN) and RNA extracted with Trizol and purified with RNeasy Mini Kit (QIAGEN). RNA was reverse transcribed to cDNA with QuantiTect Reverse Transcription Kit (QIAGEN). cDNA samples synthesized from 1μg of total RNA were subjected to PCR amplification or qRT-PCR with primers listed in Supplemental Table S1.

### SINGLE FIBER CULTURE ASSAYS

Single myofibers were prepared from the EDL muscles from 6 weeks-old C57/Bl6 or Myf5nLacZ/+ mice (3, 4) as described (5). Briefly, muscles were dissected and digested in 2% (w/v) collagenase type 1 (Sigma) in DMEM (Gibco) for 1.5 h in a 35°C water bath. Myofibers were isolated by gentle trituration of the muscle using a customized heat-polished Pasteur pipette. Individual intact myofibers were washed by serially transferring them through three dishes of warmed DMEM supplemented with 4 mM L-glutamine (Sigma) and 1% penicillin and streptomycin solution (Sigma). Then they were either plated on matrigel coated wells of a 24 wells plate in proliferating medium (20% FBS, 10% HS, 1% CEE in DMEM) or in HS coated round bottom eppendorf tubes and incubated with or without soluble recombinant mouse Cripto (see above), for 72 hrs in low activation medium (10% HS, 0.5% CEE in DMEM) and infected at a MOI of 10 with a lentiviral vector Lenti-Cripto-Ires-GFP encoding a membrane-bound form of Cripto (mCripto; Lenti-mCripto) or a control Lenti-GFP (Lenti-

Control), o/n in proliferation medium. The Cripto lentiviral vector (in pRRLsin.PPT.CMV.NTRiresGFPpre) was generated and prepared as described previously (6). The final MOI was $5x10^7$ TU/ml.

Immunofluorescence staining on C57/Bl6 fibers was performed after 72 hrs of treatment using antibodies specific for MyoD (1:50, Dako or Santa-Cruz), Pax7 (1:10, DSHB) (7), Myogenin (1:50, BD Pharmingen) and Ki67 (1:250, Abcam) (8).

Alternatively, Myf5nLacZ/+ myofibers were plated on a feeder layer of mammalian cells expressing membrane-bound Cripto or a mock vector, in 24 multiwell plate in proliferating medium (20% FBS, 10% HS, 1% CEE in DMEM). LacZ staining was performed after 72 hrs to identify activated satellite cells both on the fibers and that have left the fiber.

## SUPPLEMENTAL REFERENCES


1. Minchiotti G*, et al.* (2001) Structure-function analysis of the EGF-CFC family member Cripto identifies residues essential for nodal signalling. (Translated from eng) *Development* 128(22):4501-4510 (in eng).
2. Minchiotti G*, et al.* (2000) Membrane-anchorage of Cripto protein by glycosylphosphatidylinositol and its distribution during early mouse development. (Translated from eng) *Mech Dev* 90(2):133-142 (in eng).
3. Beauchamp JR*, et al.* (2000) Expression of CD34 and Myf5 defines the majority of quiescent adult skeletal muscle satellite cells. (Translated from eng) *J Cell Biol* 151(6):1221-1234 (in eng).
4. Montarras D*, et al.* (2005) Direct isolation of satellite cells for skeletal muscle regeneration. (Translated from eng) *Science* 309(5743):2064-2067 (in eng).
5. Rosenblatt JD, Lunt AI, Parry DJ, & Partridge TA (1995) Culturing satellite cells from living single muscle fiber explants. (Translated from eng) *In Vitro Cell Dev Biol Anim* 31(10):773-779 (in eng).
6. Brunelli S, Relaix F, Baesso S, Buckingham M, & Cossu G (2007) Beta catenin-independent activation of MyoD in presomitic mesoderm requires PKC and depends on Pax3 transcriptional activity. (Translated from eng) *Dev Biol* 304(2):604-614 (in eng).
7. Zammit PS*, et al.* (2004) Muscle satellite cells adopt divergent fates: a mechanism for self-renewal? (Translated from eng) *J Cell Biol* 166(3):347-357 (in eng).
8. Abou-Khalil R*, et al.* (2009) Autocrine and paracrine angiopoietin 1/Tie-2 signaling promotes muscle satellite cell self-renewal. (Translated from eng) *Cell Stem Cell* 5(3):298-309 (in eng).

**Figure S1. Cripto expression decreases as the regeneration process proceeds. Related to Figure1**

(A) Cripto expression in living cells derived from digested wild type muscle at day 4 after CTX injection. FACS histogram plot of cells stained with isotype-matched antibodies as negative control (left panel). Cripto positive cells were gated using Cripto APC-conjugated antibodies (right panel, P1 population), indicating that 16.2% of the cell population expressed Cripto. (B) Histogram of F4/80 (FITC) positive cells (P2 population) gated on P1 population (Cripto APC), showing that 15.2% of Cripto positive cells are macrophages. (C) ELISA-based assay measuring Cripto protein level in total protein extract of muscles at different time points after CTX injection; the average pg/mg muscle is plotted for each group at the indicated time points. Endogenous Cripto protein was detected in muscle tissue extracts at day 4 after injury (≈ 20pg/mg), whereas it decreased beyond detection levels from day 8 onward. (D-F) Representative pictures of CTX-injured muscles at indicated days after injury, stained by immunohistochemistry with anti-Cripto antibodies revealed by DAB coloration, showing that Cripto expression decreases during regeneration. Muscles are counterstained by Haematoxilin. Scale bars represent 50 μm.

**Figure S2. Cripto expression persisted in proliferating activated satellite cells. Related to Figure2**

(A-L) Cripto staining on teased myofibers isolated from Myf5-LacZ mice, at 48 hrs (A-D) or 60 hrs in culture (E-L), showing co-expression of Cripto with β-gal/ Myf5 (A-C), Pax7 (E-G), MyoD (I-K). All the images are superimposed on a phase-contrast image (D, H and L). Scale bars= 50 μm.

**Figure S3. Adenovirus –mediated sCripto overexpression *in vivo*. Related to Figure 4**

(A-D) sCripto overexpression in CTX -injected skeletal muscles infected with either Ad-sCripto or Ad-Control. (A) ELISA-based assay measuring sCripto protein level in mice serum at different time points post-adenovirus delivery; the average ng/ml serum is plotted for each group at the indicated time points. (B) ELISA-based assay measuring sCripto protein level in total protein extract of skeletal muscles harvested 6 days after CTX injection. Injured muscles were injected with increasing concentration of Ad-sCripto ($6*10^8$ - $6*10^9$pfu/ml). Adenovirus encoding empty vector has been used as control (Ad-Control) at the highest concentration ($6*10^9$pfu/ml). Ad-Control 0 vs Ad-sCripto: 0.23 ± 0.06 ng/mg at $6*10^8$pfu/ml, 0.83 ± 0.04 ng/ml at $3*10^9$pfu/mg and 2.12 ± 0,5 ng/mg at $6*10^9$pfu/ml. Values are mean ± SEM, n=3 mice/time point. (C) ELISA-based assay measuring sCripto protein level in the serum: Cripto protein is undetectable in Ad-Control -infected mice, whereas it accumulates in Ad-sCripto treated mice, decreasing with time. Cripto was undetectable in the serum of uninjured mice. (D) Immunofluorescence analysis on skeletal muscle sections at day 8 after CTX injection in the same mice, showing Cripto overexpression in Ad-sCripto treated mice compared to Ad-Control and negative control of immunofluorescence. Nuclei were stained with DAPI. Scale bars represent 50 μm.

**Figure S4. Cripto overexpression enhances muscle regeneration after injury and does not largely affect inflammation. Related to Figure 4 and 5.**

(A-B) Centrally nucleated myofibers significantly increased in Ad-sCripto treated muscles compared to control (Ad-Control) in mouse models of either hindlimb ischemia (MLI), 7 days after ligation (A) or CTX ($10^{-5}$M) 7 days after injury (B). Results are expressed as percentage of total section area. Values are the mean ± SEM, 5 mice per group, **P=0.002 for MLI and

*P<0.05 for CTX. (C) Cross sectional area (CSA) analysis of regenerated fibers in model of less severe muscle damage ($10^{-5}$M CTX), showing increased myofiber size in Ad-sCripto treated mice compared to control. (D) Quantitative analysis of F4/80 positive cell area in mice treated with Ad-sCripto vs Ad-Control at day4, 8 and 22 (3.7 ± 2% after Ad-sCripto vs 4.6 ± 1% after Ad-Control at day 4; 9.1 ± 4% after Ad-sCripto vs 5.2 ± 3% after Ad-Control at day 8; 5.7 ± 2% after Ad-sCripto vs 6.9 ± 3% after Ad-Control at day 22; n=5 mice/group; P=NS; n=5 mice/group; P=NS). Values are mean ± SEM, 5 mice/time point. (E) PCR genotyping of TA muscle and bone marrow DNA from *Tg:Pax7-CreERT2::Cripto*$^{loxP/-}$ and *Cripto*$^{loxP/-}$ mice treated with tamoxifen.

**Figure S5. GPI-anchored Cripto protein (mCripto) promotes myoblast proliferation and antagonizes Myostatin/GDF8 signaling pathway. Related to Figures 6 and 7**

A) Co-immunostaining of isolated myofibers infected with Lenti-mCripto or Lenti-control after 72 hrs in culture, show increased number of Pax7-/MyoD+ myogenic cells in Lenti-mCripto fibers compared to control (red bars, n=3 independent experiments, *P<0.01 and **P<0.001 compared to control). (B-C) Cripto antagonizes GDF8 signaling pathway. (B) Representative picture of Western Blot analysis of total lysates of C2C12, transfected with empty- or sCripto-vector and treated with increasing doses of recombinant GDF8 protein (2,5-10 nM, R&D; left panel). Densitometric analysis is expressed in arbitrary units (ADU) as P-Smad2/Smad2 ratio, and is representative of two experiments (right panel). (C) Representative picture of Western Blot analysis of total lysates of 293 cells, transfected with empty- or mCripto-vector and treated with increasing doses of recombinant GDF8 protein (2,5-10 nM, R&D). Anti -P-Smad2, -Smad2 or -Cripto antibodies were used. (D) Expression of Cripto (E) Myostatin in TA muscles at day4, 8 and 22 after CTX injection, as shown by qRT-PCR. mRNA expression

was normalized to β-tubulin expression; data are mean ± SE, n=3. See also Table S1**.**

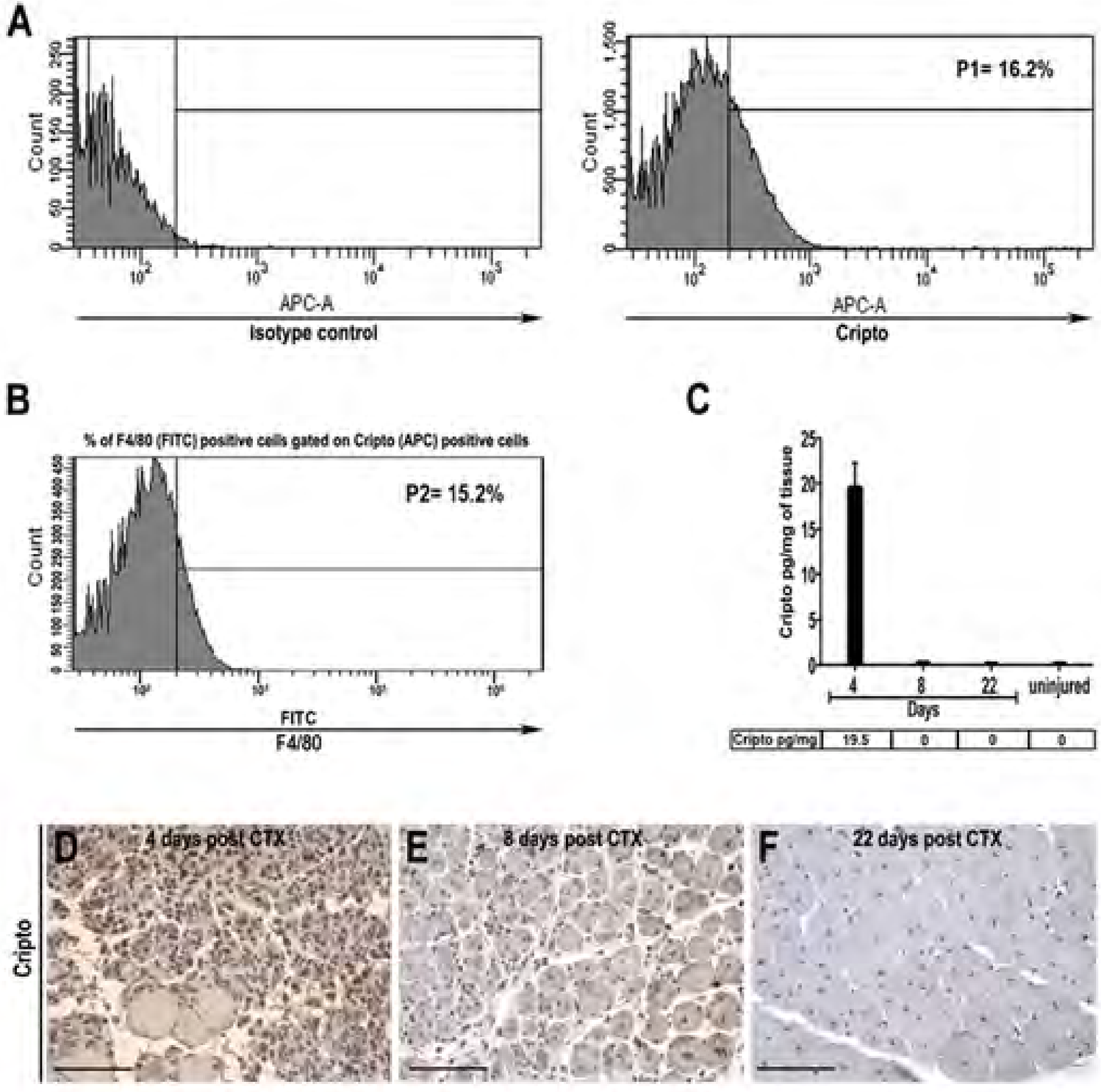
A
Count
APC-A
Isotype control
P1= 16.2%
Cripto
B
% of F4/80 (FITC) positive cells gated on Cripto (APC) positive cells
P2= 15.2%
FITC
F4/80
C
Cripto pg/mg of tissue
4
8
22
uninjured
Days
Cripto pg/mg
19.5
0
0
0
Cripto
D
4 days post CTX
E
8 days post CTX
F
22 days post CTX

Figure S1

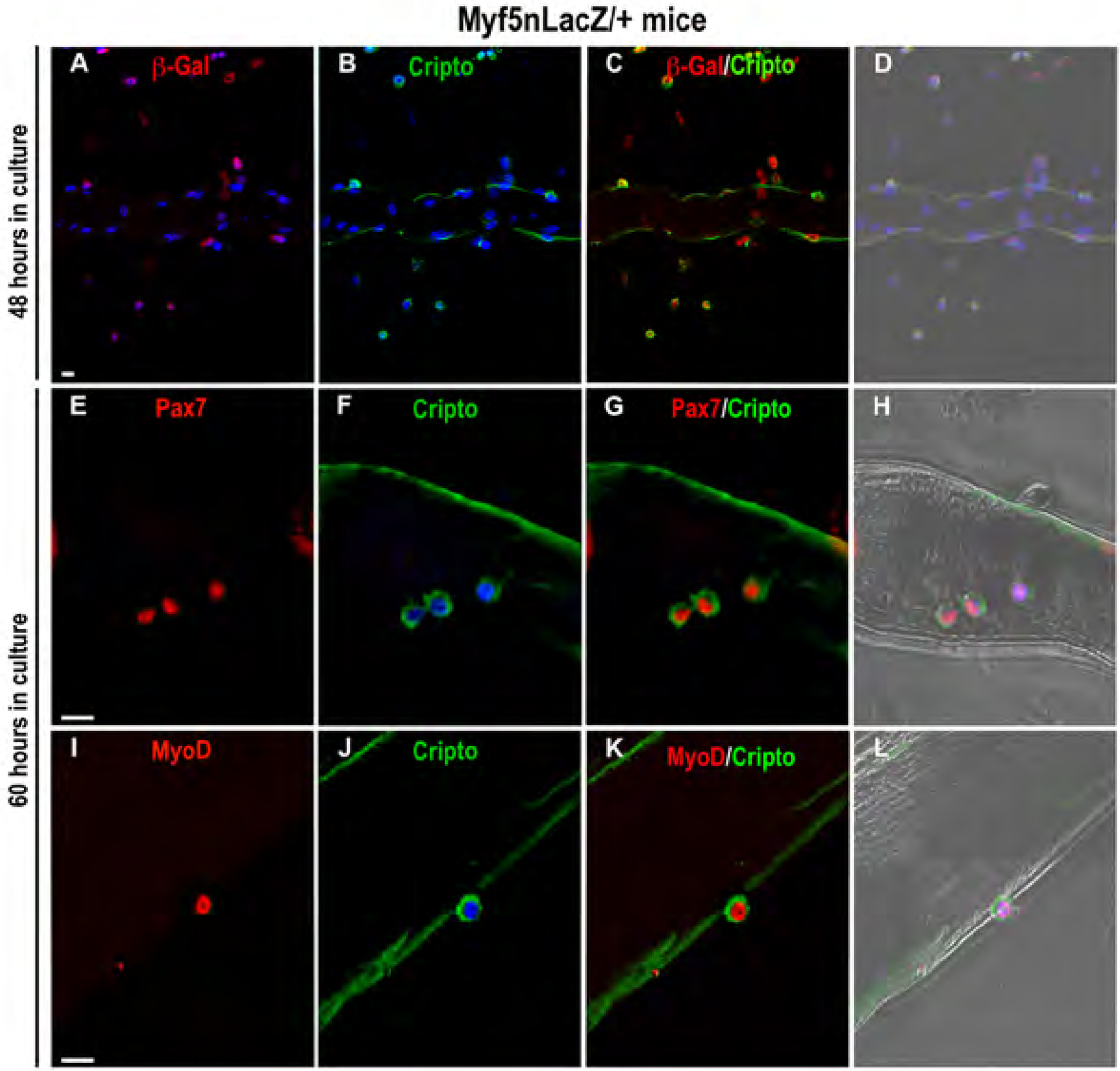
Myf5nLacZ/+ mice
48 hours in culture
60 hours in culture
A
β-Gal
B
Cripto
C
β-Gal/Cripto
D
E
Pax7
F
Cripto
G
Pax7/Cripto
H
I
MyoD
J
Cripto
K
MyoD/Cripto
L

Figure S2

A

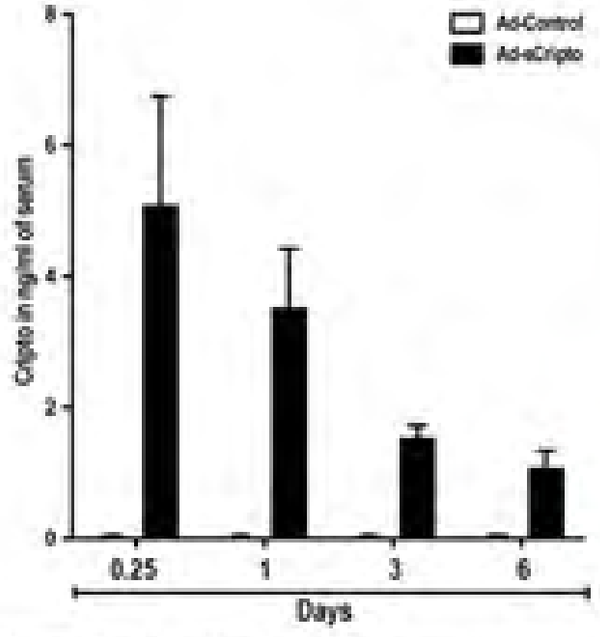


| | | | | |
|---|---|---|---|---|
| Ad-Control | 0 | 0 | 0 | 0 |
| Ad-sCripto | 5.068 | 3.489 | 1.514 | 1.055 |

B

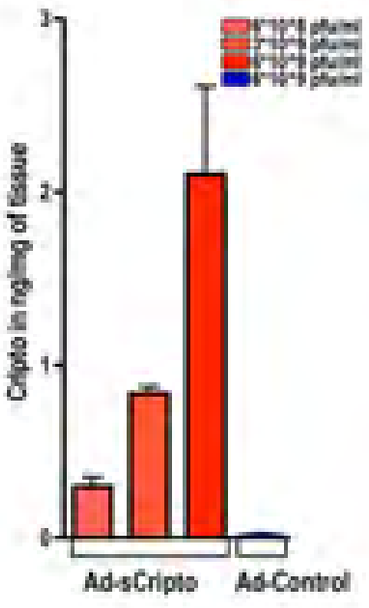


C

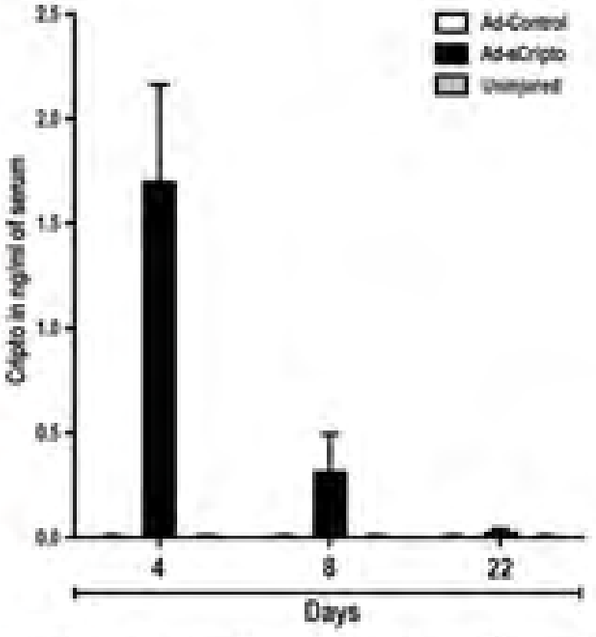


| | | | |
|---|---|---|---|
| Ad-sCripto | 1.696 | 0.313 | 0.021 |
| Uninjured | 0 | 0 | 0 |

D

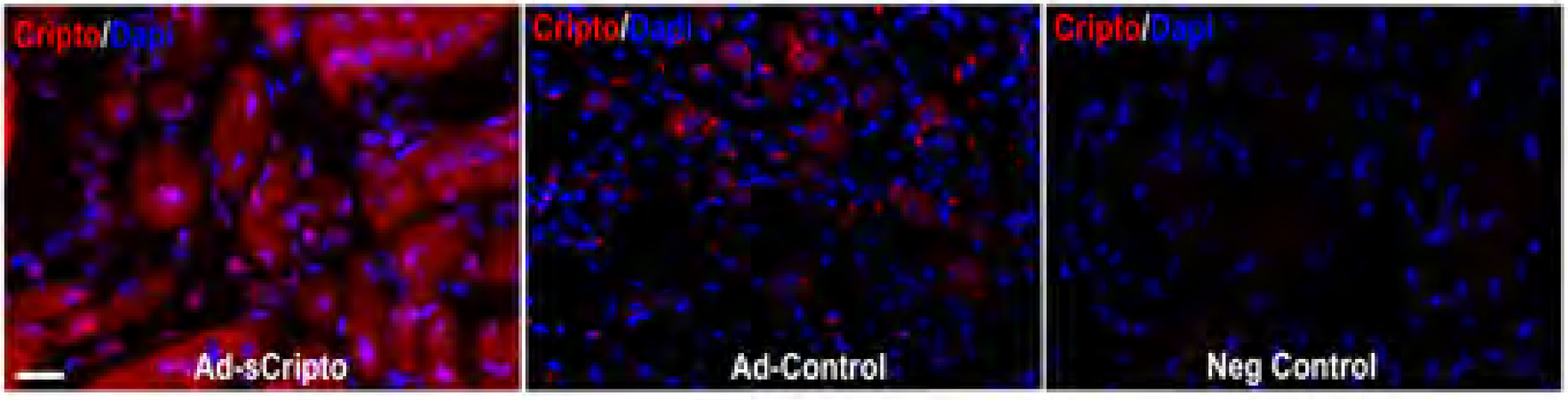


Figure S3

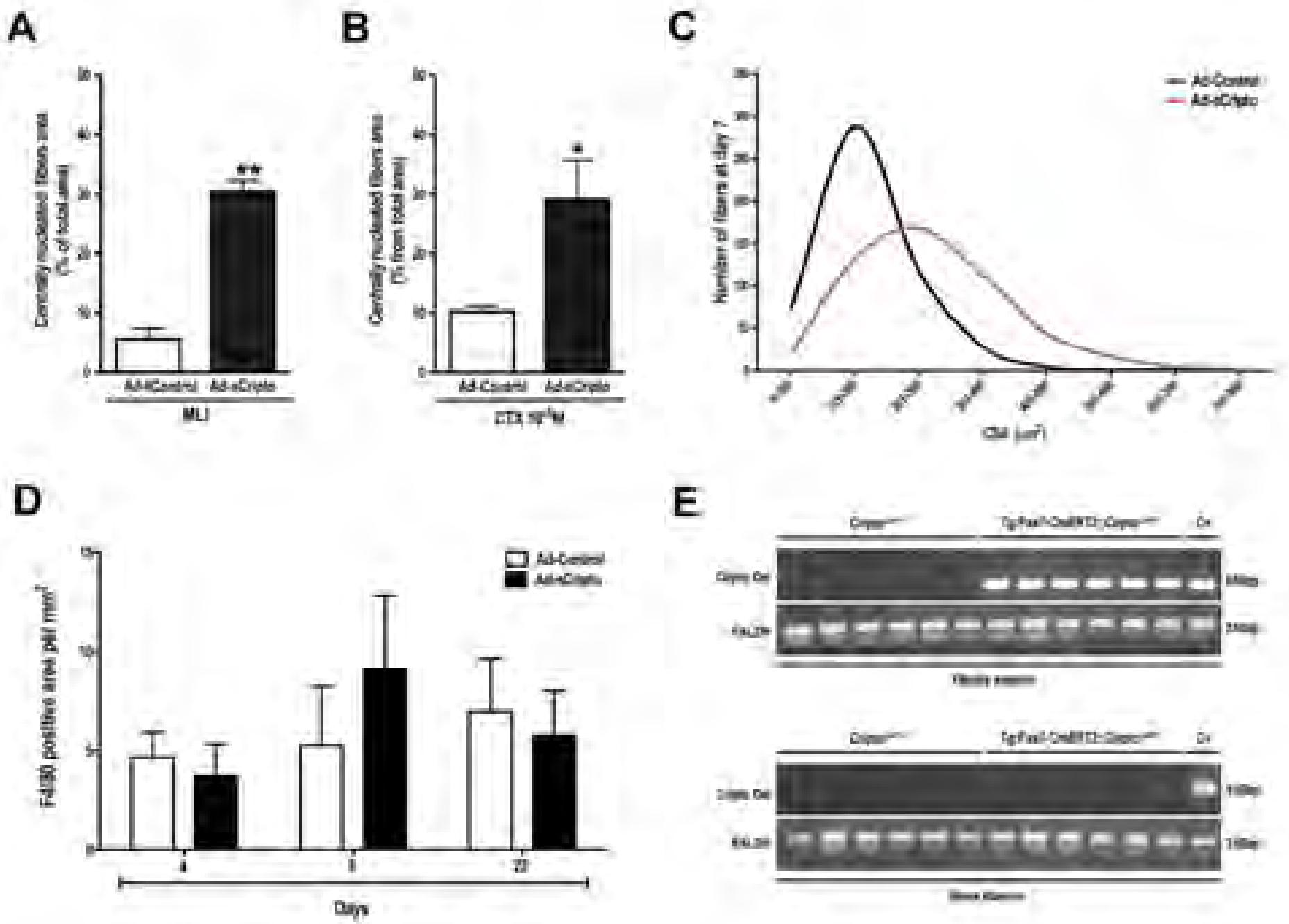


Figure S4

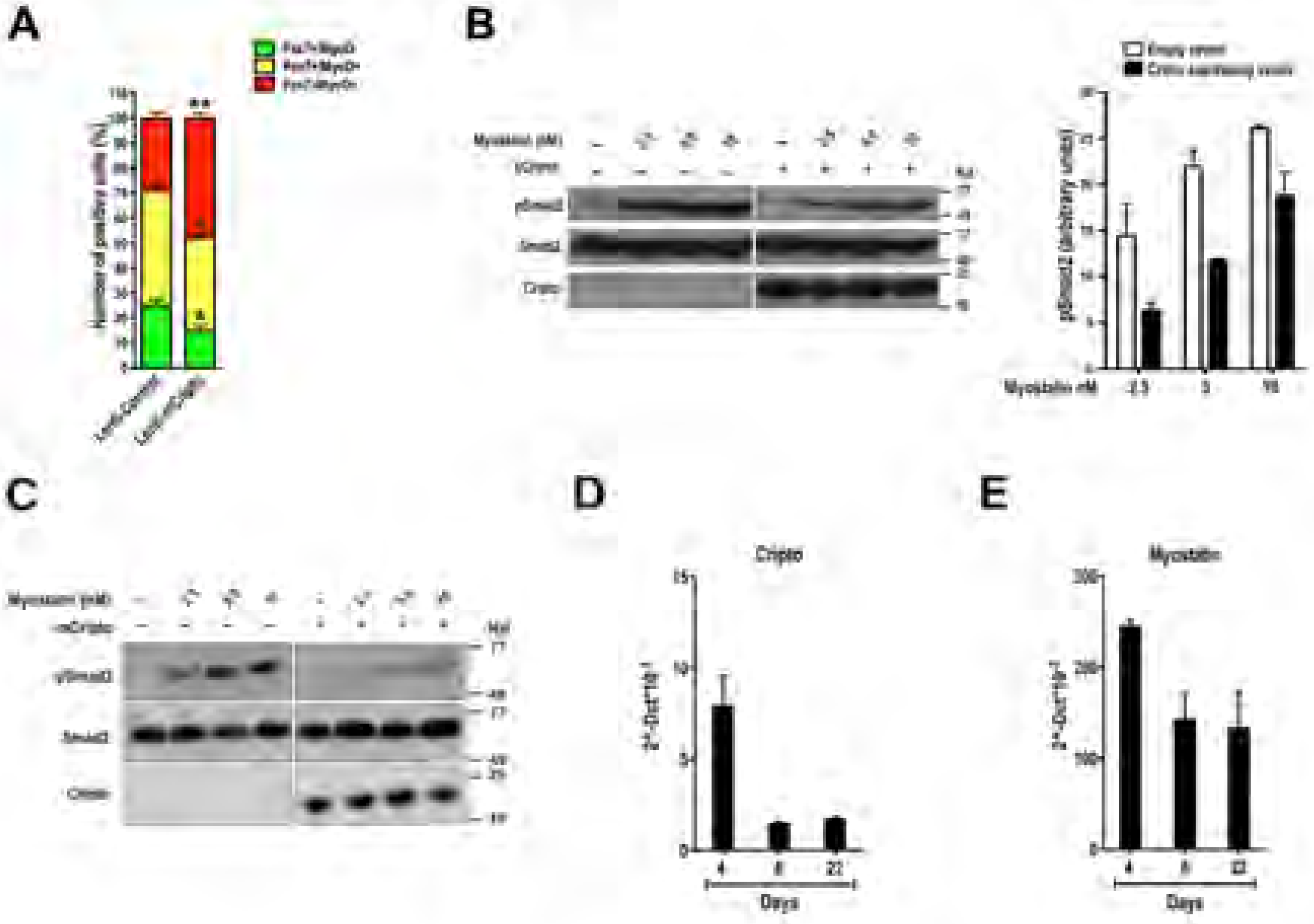


Figure S5

| **Gene** | **Primer** (**forward**) 5'-3' | **Primer (reverse)** 5'-3' |
|---|---|---|
| β-tubulin | GGGAGGTGATAAGCGATGAA | CCCAGGTTCTAGATCCACCA |
| nMyHC | GAACTTGAAGGAGAGGTCGA | CACCTTCGCCTGTAATTTGTC |
| Cripto | TGTTCGCAAAGAGCACTGTGG | TGAGGTCCTGGTCCATCACTTGAC |
| Myostatin | TGTAACCTTCCCAGGACCAG | TCTTTTGGGTGCGATAATCC |

**TABLE S1, related to Figures 4 and S5.** Primer sequences used for qRT PCR and PCR analysis.

| **Genotype** | **Primer** (**forward**) 5'-3' | **Primer (reverse)** 5'-3' |
|---|---|---|
| *Pax7CreERT2* | GAATTCCCCGGGGAGTCGCATCCTG | CCACACCTCCCCCTGAACCTGAAAC |
| LoxP/- | TCTGCACTGGGGCTAAACCTTATG | 1.GCCAAGAGCCATGACAGAGATGG<br>2. AGCGCATGCTCCAGACTGCCTT |
| Cripto Del | AGCCATCTCACCAGCCTTCA | CATCTGGGACATGCCCACTA |
| Raldh | TATCTGGACAGTGGTTAAGG | CCCAGCCTGCATAATACCTC |

**TABLE S2, related to Figures 3.** Primer sequences used for genotyping strategies.